

Wilfrid Laurier University

Scholars Commons @ Laurier

---

Theses and Dissertations (Comprehensive)

---

2020

## Characterizing the hydrological function of treed bogs in the zone of discontinuous permafrost

Brenden Disher

brendendisher1@gmail.com

Follow this and additional works at: <https://scholars.wlu.ca/etd>



Part of the [Hydrology Commons](#)

---

### Recommended Citation

Disher, Brenden, "Characterizing the hydrological function of treed bogs in the zone of discontinuous permafrost" (2020). *Theses and Dissertations (Comprehensive)*. 2261.

<https://scholars.wlu.ca/etd/2261>

This Thesis is brought to you for free and open access by Scholars Commons @ Laurier. It has been accepted for inclusion in Theses and Dissertations (Comprehensive) by an authorized administrator of Scholars Commons @ Laurier. For more information, please contact [scholarscommons@wlu.ca](mailto:scholarscommons@wlu.ca).

# **Characterizing the hydrological function of treed bogs in the zone of discontinuous permafrost**

by

Brenden S. Disher

(B.A. Geography, Wilfrid Laurier University, 2017)

THESIS

Submitted to the Department of Geography and Environmental Studies  
in fulfilment of the requirements for  
Master of Science in Geography

Wilfrid Laurier University

© Brenden Disher 2019

## ABSTRACT

The loss of permafrost has produced a wholesale conversion from forest to wetland, and many studies have analyzed the effects of permafrost thaw-induced land cover change on the hydrology and ecology of landscapes within the Taiga Plains. The permafrost thaw driven areal shrinkage of forested plateaux and their replacement by treeless wetlands is well documented, and the co-occurrence of permafrost and black spruce forest cover is the basis for areal estimates of the former. However, field studies conducted at a peatland dominated landscape near Fort Simpson, NWT indicate that tree canopy may persist following the loss of permafrost and the gradual drying and succession of the previously treeless bog landscape. Such treed bogs are present on the borders of thawed plateaux and within larger and more established bog complexes. These features are typically characterized by stunted black spruce (*Picea mariana*), ground lichen (*Cladonia* spp.), and sphagnum hummocks (*Sphagnum* Spp). A total of four sites, each containing a bog, treed bog and peat plateau were chosen based on a supervised image classification completed within the basin. A geophysical investigation was completed to determine permafrost presence, depth of seasonal ice was measured along transects at each site, a series of wells were installed to measure hydrological response and discrete soil moisture measurements were taken immediately following snowmelt to characterize differences in moisture retention. Treed bogs are permafrost free features that intersect peat plateaux and bogs in terms of their hydrology. It is not clear whether these features represent a temporary state of succession for drier bogs, or if they will remain as permanent features on the landscape. Understanding the succession of northern landscapes due to climate warming provides an important step in predicting the trajectory of change in the north. This work provides new insights regarding the future of post-thaw landscapes within the Taiga Plains.

**Keywords:** permafrost thaw, landscape transition, hydrology, cold regions, climate warming, Scotty Creek

## **ACKNOWLEDGEMENTS**

First and foremost, I would like to thank my supervisor Dr. Bill Quinton for his guidance and mentorship throughout this project. I am incredibly grateful for the encouragement and enthusiasm that he has offered my work. I would also like to thank Dr. Ryan Cannon for his continued support, guidance, and mentorship in (and out) of the field throughout the entirety of this project, as well as Dr. Chris Hopkinson and Dr. Jonathan Price for their help with the preparation of this thesis.

I would also like to thank the many Scotty Creek researchers and members of the Quinton Lab for all their help over the last two years. A special thanks to Jessica Smart, Mason Dominico, Olivia Carpino, Kristine Haynes, and Angela Elgie. You all helped and encouraged me through some of the more challenging problems I've faced over the last two years; I don't know what I would have done without your much-needed help - Thank you.

Finally, I would like to thank my friends, family, and most importantly my partner Bernadette, who stood by my side the last two years. Your endless support and encouragement have allowed me to get to where I am today.

## List of Figures

**Figure 1:** (a) Location of Scotty Creek, located 50km south of Fort Simpson, NWT. (b) Aerial imagery (Worldview-2) with each geophysical transect, soil moisture transects, and well locations plotted at each study site. (c) Each treed bog feature (sites 1-4) highlighted with high-quality ortho-mosaic imagery..... 39

**Figure 2:** Electrical Resistivity Tomography (ERT) transects for site 1. (a) Transect 1 (83m) includes all three landcover types, (b) Transect 2 (28m) measures Treed bog. Note difference in scale between the two plots measurements were completed in August 2018 ..... 40

**Figure 3:** SWE and SCA measurements. SWE. Snowmelt commences on April 23rd and is denoted by the dotted line. Pre-melt measurements were taken for approximately 15 days, while melt measurements were taken for 5 days. The error bars represent the standard deviation of the average SWE measurement for each landcover type. After the final measurement (April 26th), linear interpolation was used to complete melt for each feature and is denoted with the dashed line. It should be noted that the snow-free day for each landcover type is approximated to  $\pm 1$  day using areal imagery and field notes, and. Snow covered area (SCA%) is plotted near the end of the period to depict the areal loss of the snowpack and is denoted by the dotted lines..... 41

**Figure 4:** Mosaiced drone images of classified snow cover for three study sites throughout the snowmelt period. Images were captured daily and were classified using an iso cluster unsupervised image classification. Snow cover for each day is depicted in light blue. April 25th is the baseline for the analysis.....42

**Figure 5:** Thickness of seasonal frost for all three land cover types. Peat plateau and treed bog were not statistically different ( $p = 0.5$ ). The thickness of seasonal frost in the treeless bog had statistically significant ( $p < 0.05$ ) differences than the other two land cover types. The notches within each boxplot represents an approximate 95% confidence interval of the median. If the notches do not overlap, there is evidence of a statistically significant difference. .... 43

**Figure 6:** a) Daily ground temperature at 10cm depth at three locations within Site 1; b) Length of the zero-curtain period for each land cover type between October 2018 and April 2019. .... 44

**Figure 7:** Continuous soil moisture VWC ( $m^3/m^3$ ) record at 5 discrete depth intervals (5cm, 10cm, 15cm, 20cm, 25cm, 30cm) for each landcover type. Data was collected for a year between June 2018 and June 2019. Data was removed at 5 cm from the treeless bog due to contact issues with the sensor, and the abrupt changes in VWC in mid-August occurred due to the sensors being disturbed and fixed less than a week later . 45

**Figure 8:** Mean water table measurements between May and June 2018 were recorded every 30-min at each well using a pressure transducer and are denoted as the solid

line. The dotted line denotes the mean ground elevation ( $n = 4$ ) surrounding each corresponding well and was measured in the summer of 2018 using dGPS. Precipitation events (greater than 0.2mm) are depicted in the first plot. The average water table depth was 9 cm at the treeless bog wells and 12.5 cm at the treed bog wells ..... 46

**Figure 9:** a) Master recession curve trendlines for each treed and treeless bog well. The single peat plateau well was not plotted due differences in magnitude. b) A summary of each individual precipitation event and its corresponding mean recession coefficient for each landcover classification.. ..... 47

**Figure 10:** Supervised image classification of Scotty Creek within a small subset of the peatland portion of the basin. The classification was completed using Worldview-2 and LiDAR imagery. .... 48

**Figure 11:** Conceptual diagram displaying differences in measured snow depth, depth of seasonal ice, and water table elevation between each landcover type, as well as the formation of treed bogs through both time and space. Currently, it is proposed that treed bogs form due to the upward growth of *Sphagnum* spp. and the gradual dewatering of landscapes. Each panel of the four panels represent the approximate season in which the data collection occurred. The arrow denoting time represents the temporal transition of landscapes, while the arrows depicting upward growth represents the spatial transition of treed bogs. All data was plotted relative to the ground elevation points. .... 49

# List of Appendix

<b>Appendix A:</b> Additional information on methods.....	67
<b>Appendix B:</b> Additional discussion .....	67
<b>Appendix C:</b> Statistical analysis of SWE, depth of refreeze and slope recession analysis. All tests were run at a 95% confidence interval. ....	67
<b>Appendix D:</b> Topographic, canopy, and spectral thresholds used for each landcover type within the image classification. Variables with dashes were not used to classify that landcover. ....	68
<b>Appendix E:</b> Confusion matrices of predicted ‘snow-free’ and ‘snow-covered’ area compared to actual ‘snow-free’ and ‘snow-covered’ area of all drone images used for the SCA analysis. Classification accuracies are presented with overall accuracy, misclassification rate, and Kohen’s Kappa. ....	69
<b>Appendix F:</b> Confusion matrix of predicted landcover type compared to actual landcover type within the classification AOI. Classification accuracies are presented with overall accuracy, misclassification rate, and Kohen’s Kappa. ....	70
<b>Appendix G:</b> Discrete soil moisture points collected between 14-May and 01-June for each landcover type (n=20). Data was collected with a hydrosense-2 handheld soil moisture probe. ....	71

# Table of Contents

<b>ABSTRACT</b> .....	ii
<b>ACKNOWLEDGEMENTS</b> .....	iii
<b>List of Figures</b> .....	iv
<b>List of Appendix</b> .....	vi
<b>CHAPTER 1.0:</b> .....	1
<b>General Introduction</b> .....	1
1.1 Introduction and background .....	1
1.2 Permafrost Degradation .....	1
1.3 Landscape Succession .....	3
1.4 Hydrology of discontinuous permafrost regions .....	4
1.5 Landscape Trajectory .....	5
<b>CHAPTER 2.0:</b> .....	8
<b>Characterizing the hydrological role of treed bogs in the zone of discontinuous permafrost, Northwest Territories, Canada</b> .....	8
2.1 Abstract .....	8
2.2 Introduction .....	9
2.3 Study Site.....	12
2.4 Methods .....	13
2.4.1 Site selection.....	13
2.4.2 Geophysical Investigation .....	14
2.4.3 Snowpack Characteristics .....	15
2.4.4 Seasonal ground freeze and thaw .....	16
2.4.5 Soil Moisture .....	17
2.4.6 Water level fluctuations and hydrograph recession .....	17
2.4.7 Image classification and analysis .....	19
2.4.8 Statistical Analyses .....	20
2.5 Results and discussion .....	21
2.5.1 Geophysical Investigation .....	21
2.5.2 Snowpack Characteristics .....	22
2.5.3 Seasonal ground freeze and thaw .....	24
2.5.4 Soil Moisture .....	26
2.5.5 Water level fluctuations and hydrograph recession .....	27

2.5.6 Image classification and analysis .....	29
2.5.7 Conceptual model of landscape succession.....	30
2.6 Conclusion .....	33
2.7 Acknowledgements .....	34
<b>CHAPTER 3.0: Conclusion and future research .....</b>	<b>35</b>
3.1 Summary and Conclusions .....	35
3.2 Future Research .....	37
<b>Figures .....</b>	<b>39</b>
<b>References .....</b>	<b>50</b>
<b>Appendix A .....</b>	<b>56</b>
<b>Appendix B .....</b>	<b>59</b>
<b>Appendix C .....</b>	<b>62</b>
<b>Appendix D .....</b>	<b>63</b>
<b>Appendix E.....</b>	<b>64</b>
<b>Appendix F.....</b>	<b>65</b>
<b>Appendix G .....</b>	<b>66</b>

# CHAPTER 1.0:

## General Introduction

### 1.1 Introduction and background

Permafrost is a product of cold climates, typically where mean annual air temperature (MAAT) is below 0°C, and can be defined as ground that remains at or below 0°C for two or more consecutive years (Mackay 1972). Permafrost distributions may be either continuous or discontinuous in nature, but within the discontinuous permafrost zone permafrost may underlie between 10% and 90% of the landscape. This zone can be further broken down into sporadic-discontinuous and extensive-discontinuous permafrost distributions. As climate warming is occurring disproportionately in northern latitudes, permafrost is experiencing increasing rates of thaw (Payette et al., 2004; Quinton and Connon, 2017). Although MAAT provides a good analogue to determine permafrost extent over a large spatial scale, distributions may be spatially limited to variables such as vegetation, soil moisture, and snow cover. For example, within the sporadic-discontinuous zone permafrost distributions are generally restricted to peatlands, where the insulative properties of the peat maintains the thermal offset required to sustain permafrost, as MAAT in sporadic-discontinuous zone typically approaches 0°C. Permafrost in these regions is typically found beneath treed peat plateaux which are raised 1-2m above the surrounding low elevation wetlands. Permafrost-free features (i.e. collapse-scar bogs and fens) within this region are low elevation, saturated, and are regarded as canopy free (Vitt et al. 1994; Beilman et al. 2001)

### 1.2 Permafrost Degradation

Permafrost degradation is defined as a natural decrease in the vertical or horizontal thickness of a permafrost body (Brown, 1970); in discontinuous permafrost peatland complexes,

it is often dominated by a combination of intense lateral and horizontal degradation to the permafrost body. As northwestern Canada rapidly warms, permafrost degradation is resulting in concomitant changes to the ecology (Baltzer et al. 2014; Shur & Jorgenson 2007), hydrology (Connon et al. 2014; Connon et al. 2015; Walvoord & Kurylyk 2016), and carbon cycling (Helbig et al. 2016) of northern landscapes, such that landscape transition is occurring rapidly (Payette et al. 2004; Quinton & Connon 2017). Ground subsidence, waterlogging, and the tilting of black spruce (*Picea Mariana*) trees are a byproduct of the intense thaw described above, and the extensive conversion of forested plateau to treeless wetland has been well documented (Robinson & Moore 2000; Quinton et al. 2011; Baltzer et al. 2014). The areal shrinkage of treed peat plateaux and their replacement by treeless wetlands has been widely observed throughout northern regions (Quinton et al. 2011; Chasmer & Hopkinson 2016; Jorgenson & Osterkamp 2005; Robinson & Moore 2000), and many studies have focused on tracking the landscape-wide implications of these changes. Earlier studies have used manual delimitation and a black spruce canopy (*Picea mariana*) as a proxy for determining permafrost distributions (Tutubalina & Rees 2001; Chasmer et al. 2010; Quinton et al. 2011), as it has been established that black spruce canopy cover typically only exists atop dry peat plateaux (Vitt et al. 1994; Beilman et al. 2001), while later studies used a combination of canopy, spectral and topographic characteristics to classify landcover types (Tutubalina & Rees 2001; Chasmer et al. 2011; Chasmer et al. 2014). Manual delimitation is often more labor intensive but less complex, as it involves outlining areas of black spruce canopy manually. Because of this, it would often overestimate the percentage of landscape that may contain permafrost. Solutions such as completing a classification using multi-spectral imagery are often more complex, but studies have noted increases in landscape classification accuracies (Nguyen et al. 2009; Chasmer et al. 2014). Nonetheless, estimates of permafrost distributions remain useful for understanding landscape change under warming climate conditions.

### 1.3 Landscape Succession

The peatlands of northwestern Canada were first established as fens following the retreat of the Laurentide ice sheet, which occurred between 8000 years and 9000 years before present (BP) (Zoltai 1993; Zoltai 1995). Bog development within this region was initiated 5000 years BP, with the first sign of permafrost occurring around 3700 years BP (Zoltai 1993). The degradation and subsequent aggradation of permafrost bodies in southern peatlands has occurred frequently since 3700 years BP, and was often triggered by a large disturbance such as a fire, with the degradation-aggradation observed to operate over a period as short as 600 years (Zoltai 1993). Currently, permafrost degradation is the dominant mechanism in northwestern Canada due to anthropogenic warming, often resulting in dramatic landscape change (Camill 2005; Jorgenson & Osterkamp 2005; Payette et al. 2004). Aggradation mechanisms are primarily driven by the succession of *Sphagnum* from aquatic species (*S. riparium*) to lawn species (*S. angustifolium*, and *S. fuscum*), the subsequent establishment of a black spruce canopy, and the insulating properties of dry *Sphagnum* peat (Vitt et al. 1994; Zoltai & Tarnocai 1975). As these successional processes occur, there is a spatial and temporal transition from inundated collapse-scar communities to that of hummocky communities that grow above the local water table (Vitt et al., 1994; Camill, 1999). The establishment of hummock terrain provides drier conditions to support the growth of black spruce saplings by preventing the inundation of the rooting network. Both the insulating properties of peat as well as the development of a canopy plays a key role in the development of permafrost, as it a For example, tight clusters of canopy cover may intercept early snowfall, allowing the frost table to penetrate to a greater depth due to the insulative properties of peat near the surface (Zhang 2005; Zoltai 1972; Camill 2000). As this process advances, the frost table may penetrate to such a depth that it does not completely thaw the following summer. Such processes have been

investigated in chronological cores at many sites throughout northern peatlands (Zoltai, 1993), and have been observed in peatland sites in southern NWT (Chasmer & Hopkinson 2016; Pelletier et al. 2017). Although it is unlikely the climate within the southern discontinuous region is in a period conducive to permafrost aggradation, the processes involved in the localized succession of the landscape may continue to operate under a warming climate.

#### **1.4 Hydrology of discontinuous permafrost regions**

Permafrost presence places a strong control on the local hydrology within the discontinuous permafrost region. For example, within regions of high relief, many studies have documented the relationship between permafrost presence and aspect, such that north facing slopes contain permafrost and produce runoff, while south facing slopes are often well-drained and permafrost free (Carey & Woo 2001; Carey & Woo 1999; Woo et al. 2008; Ishikawa et al. 2005). Within the peatland portion of the discontinuous permafrost zone, relief is low, and therefore the permafrost presence is a function of the insulating properties of vegetation (Brown 1970), such that each landcover type has a distinct hydrological function on the landscape (Quinton et al. 2003; Hayashi et al. 2004; Wright et al. 2008). The scope of this work is limited to low-relief peatlands within the sporadic-discontinuous permafrost zone. Peat plateaux are elevated features that, during high yield events such as snowmelt, will direct large quantities of runoff into lower elevation features due to the steep elevational gradient and hillslope runoff processes (Wright et al. 2008). Because of this, landcover induced gradients between peat plateaux and low elevation features are prevalent throughout peatland complexes. Runoff from peat plateaux is highest during spring snowmelt due to the increased availability of water and shallower frost table depths allowing the water table to occupy a zone of uniformly high hydraulic conductivity (Wright et al. 2008; Quinton et al. 2009), and lowest in the summer as they are often in a moisture deficit throughout the summer period. Collapse-scar wetlands are

low elevation storage features within the basin, as they receive inputs from either precipitation or runoff from higher elevation peat plateaux, which is then retained as storage, lost to evaporation, or routed laterally through a series of connected collapse-scar wetlands (Hayashi et al., 2004; Wright et al., 2009; Connon et al., 2015). Runoff from collapse-scar wetlands is typically limited due to the very low hydraulic conductivity of the permafrost bodies that surround them. Drainage channels between bogs within discontinuous permafrost peatlands have been observed in both northern Manitoba and Alberta (Thie 1974; Vitt et al. 1994), but were recently quantified within Scotty Creek by following a modified conceptual runoff model of 'fill-and-spill' proposed by Spence and Woo (2003). Because it was hypothesized that runoff between bogs could only occur during high yield events, it was suggested a 'threshold concept' be utilized, such that runoff between cascading bogs can only occur if the storage capacity of the upstream bog is first met (Connon et al. 2015). It is hypothesized that increases to the runoff contributing area occur following the loss of permafrost (Connon et al. 2015), resulting in lower elevation peripheral channels that cascade several collapse-scar bog features during high-yield events contributing to the basin drainage network (Connon et al. 2015; Haynes et al. 2018). The near-surface water table and saturated conditions typically present within collapse-scar bogs may prevent the establishment of a canopy cover. Flow in the headwaters of the Lower Liard river valley is typically restricted to channel fens (Hayashi et al. 2004). These features are typically bordered by peat plateau's and transport water to the basin outlet.

## **1.5 Landscape Trajectory**

As air temperatures rise and discontinuous permafrost peatlands experience further degradation, increasing hydrologic connectivity between landscapes and the succession of *Sphagnum* communities within larger bog complexes may provide ideal conditions for the establishment of canopy, such that the re-emergence of canopy cover is an important and

emerging trend within northern peatlands (Murphy et al. 2009; Kettridge et al. 2013; Waddington et al. 2015). Several studies have suggested both climate warming in northern peatlands and the anthropogenic drainage of temperate peatlands may lead to the re-establishment of shrub and canopy conditions (Jeglum & He Fangliang 1995; Pellerin & Lavoie 2000; Lohila et al. 2011; Waddington et al. 2015), while studies within the discontinuous permafrost zone have suggest similar trends due to dewatering and landscape succession (Ketteridge *et al.*, 2013; Chasmer and Hopkinson, 2016; Carpino *et al.*, 2018) . Carpino et al., (2018) examined forest growth and reduction along a latitudinal gradient (58 – 62°N) and found that peatlands below 60° N experienced forest expansion rather than loss whereas the dominant process above this parallel was canopy loss. It is hypothesized that this growth is driven by landscape-scale drying, while the canopy loss above 60°N is driven by permafrost thaw, and that such landscape succession occurring below 60°N will shift northward with rises in mean annual air temperature. Similar trends in runoff and canopy loss have also been noted within the broader Taiga Plains (Connon et al. 2014; M. Helbig et al. 2016; Chasmer & Hopkinson 2016). Additionally, Vitt et al. (1994) analyzed the stratigraphy of bogs within peatlands of three Canadian provinces, and found drier conditions present within bogs containing hummocky *Sphagnum spp.* that were capable of supporting small black spruce trees. Further, studies completed in the sporadic-discontinuous permafrost region have noted decreases in the water levels of hydrologically connected bogs over a 15-year period (Haynes et al. 2018), while a study within the same region noted landscape-wide canopy re-emergence in areas that have already experience significant permafrost thaw (Chasmer & Hopkinson 2016). Currently, it is hypothesized that a combination of landscape-wide dewatering and successional processes within bogs are leading to the re-establishment of canopy cover.

Recent field observations at Scotty Creek Research station (SRCS) suggest that canopy cover may exist independently of permafrost distributions. The exact mechanism leading to the

formation of treed bogs remains unclear, but it is hypothesized that these features formed following the succession of a previously thawed landscape. Regardless, understanding the succession of northern landscapes under a warming climate provides an important step in understanding the trajectory of northern peatlands. Other studies have examined the transition from treed peat plateaux to treeless collapse-scar wetlands or “*treeless bogs*”, but few have examined the re-establishment of canopy of northern peatlands. This research seeks to gain a more thorough understanding of treed collapse-scar wetlands or “*treed bogs*” within the discontinuous permafrost zone, as well as provide insights regarding post thaw landscapes within discontinuous permafrost peatlands. This research question is analyzed and addressed through four key research objectives:

- 1) Determine ground ice presence or absence beneath treed bogs, as it is currently unknown as to whether treed bogs contain permafrost.
- 2) Examine variations in the snowpack retention, depth of refreeze, soil moisture, and water level of treed bogs compared to more well-studied landcover types such as treeless bogs and peat plateaux.
- 3) Determining both the presence and spatial extent of treed bogs within in a small are of interest based on their spectral and physical properties derived from remotely sensed datasets, and
- 4) Present a conceptual diagram described the formation and significance of treed bog formation on the landscape.

## CHAPTER 2.0:

### Characterizing the hydrological role of treed bogs in the zone of discontinuous permafrost, Northwest Territories, Canada

#### 2.1 Abstract

Permafrost loss in the Taiga Plains has produced a wholesale conversion from forest to wetland, and many studies have analyzed the effects of permafrost thaw-induced land cover change on the hydrology and ecology of landscapes, such that the shrinkage of forested plateaux and their replacement by treeless wetlands is well documented. However, field studies conducted at a peatland dominated landscape near Fort Simpson, NWT indicate that tree canopy may persist within locally elevated collapse-scar wetlands. Such treed bogs are present on the borders of thawed plateaux and within larger and more established bog complexes. These features are typically characterized by stunted black spruce (*Picea mariana*), ground lichen (*Cladonia* spp.), and sphagnum hummocks (*Sphagnum* spp). A total of four sites, each containing a bog, treed bog and peat plateau were selected based on field visits and inspection of areal imagery. A geophysical investigation was completed to determine permafrost presence, depth of seasonal ice was measured along transects at each site, a series of wells were installed to measure hydrological response and discrete soil moisture measurements were taken immediately following snowmelt to characterize differences in moisture retention. Treed bogs are permafrost free features that intersect peat plateaux and collapse-scar bogs in terms of their hydrology, and its hypothesized they formed following the colonization of hummock forming *Sphagnum* spp. and the gradual dewatering of peatlands. Understanding the succession of northern landscapes due to climate warming provides an important step in predicting the trajectory of change in the north. This work provides new insights regarding the future of post-thaw landscapes within the Taiga Plains.

## 2.2 Introduction

Climate warming in northwestern Canada is leading to rapid permafrost degradation and changes to both the cycling and storage of water and energy (Quinton et al. 2011; Shur & Jorgenson 2007). Rates of climate warming are highest in arctic and sub-arctic regions (Payette et al. 2004; Tarnocai 2009), and as a result, these regions are particularly vulnerable to permafrost thaw and the associated landscape transitions (Camill 2005).

Peatlands occupy 12 percent of Canada, nearly all of which (97%) are located in the sub-arctic and boreal regions (Tarnocai 2009). The discontinuous permafrost region occurs where the mean annual air temperature (MAAT) is between 0° and -5° C (Osterkamp & Romanovsky 1999). Where its occurrence is discontinuous or sporadic, permafrost is restricted to relatively dry organic-covered terrains which can maintain the large thermal offset required to sustain permafrost, where the MAAT approaches (Halsey *et al.*, 1995) or even exceeds (Halsey et al. 1995; Shur & Jorgenson 2007) 0°C. In this environment, permafrost typically occurs below peat plateaux, which are raised 1 to 2 m above the surrounding permafrost-free, treeless wetlands including channel fens and collapse-scar wetlands (Beilman 2001; Vitt et al. 1994). The slightly higher elevation of the plateaux allows them to maintain an unsaturated layer and therefore sufficiently dry conditions to support a mature black spruce (*Picea mariana*) canopy (Vitt et al. 1994; Beilman et al. 2001). However, permafrost thaw results in subsidence, inundation of the plateau ground surface, and loss of the tree canopy (Zoltai 1993; Beilman 2001; Quinton et al. 2011; Baltzer et al. 2014)

In discontinuous permafrost regions, permafrost bodies below peat plateaux thaw by the deepening of the permafrost table (vertical thaw) and by the recession of their edges (lateral thaw) (Jorgenson et al. 2010; Walvoord & Kurylyk 2016), while the formation of a supra-permafrost talik may enable permafrost thaw throughout the entire year (Connon et al. 2018). Zoltai (1993) described a cyclical process whereby plateaux develop within permafrost free

treeless wetlands, and after a period of several centuries, develop low elevation collapse-scar wetlands. Throughout this process, the relative proportions of permafrost and permafrost-free terrains were assumed to remain relatively constant. However, climate warming in recent decades has disrupted this balance such that the rate of permafrost loss greatly exceeds the rate of permafrost development. Permafrost thaw results in ground surface subsidence, inundation, and loss of canopy cover (Baltzer et al. 2014), and ultimately a conversion of forest to wetland with implications to drainage processes and pathways (Connon et al. 2014, 2015), ecology (Baltzer et al. 2014), and carbon cycling (Helbig et al. 2016), and biogeochemical cycling (Gordon et al. 2016).

Recent studies have identified specific mechanisms by which permafrost thaw affects water flux and storage processes. For example, Connon et al. (2014) described the process of 'bog capture' whereby permafrost thaw and resulting subsidence of the terrain enables wetlands to coalesce. In other cases, wetlands may remain as distinct features, but permafrost thaw may generate ephemeral flow path between wetlands, allowing water to drain from one to the other along a cascade of hydrologically connected wetlands (Connon et al. 2015). Permafrost thaw therefore increases the hydrological connectivity among wetlands (Quinton et al. 2019), the runoff contributing area (Connon et al. 2015), and the annual basin runoff (Haynes et al. 2018). Recent studies also suggest that continued permafrost thaw is leading to the gradual dewatering of northern peatlands (Quinton & Connon 2017; Waddington et al. 2015; Haynes et al. 2018; Quinton et al. 2019), which may allow the re-establishment of canopy cover (Ketteridge *et al.*, 2013; Chasmer and Hopkinson, 2016; Carpino *et al.*, 2018).

At Scotty Creek, Northwest Territories (NWT), Canada, treed collapse-scar wetlands occur between permafrost plateaux and permafrost-free treeless wetlands (Quinton et al. 2019). The relatively young age of their trees (Haynes et al. *in prep*) suggests that treed collapse-scar wetlands evolve from treeless wetlands rather than from peat plateaux (Carpino et al. *in prep*).

The mechanisms for this transition, described by Zoltai (1993) are driven by the succession of *Sphagnum spp.* communities, the establishment of a black spruce (*Picea mariana*) canopy, and the insulating properties of *Sphagnum* peat-forming communities (Halsey et al. 1995). As *Sphagnum* communities succeed from aquatic species (*S. riparium*) to lawn species (*S. angustifolium*, and *S. fuscum*), there is an evolution from inundated aquatic or lawn communities to that of raised hummock communities (Camill, 1999). As these communities' change, they elevate the ground surface above the local water table, acting as a refuge for black spruce saplings. The very low thermal conductivity of dry peat limits thaw during summer, while the relatively shallow snow depth over hummocks within clusters of canopy enables greater ground cooling during winter and conditions favourable for permafrost aggradation (Shur & Jorgenson 2007; Zoltai 1993). Although ice lenses and permafrost provide dry conditions necessary for tree growth, the drying of collapse-scar wetlands, and the vertical growth of *Sphagnum* communities may also provide conditions that are favorable to the growth of a black spruce tree. The processes described above allow for the formation of such treed collapse-scar wetlands appear to persist in a collapse-scar bog landscape that would previously be unable to maintain trees.

The rate and pattern of the wetland to forest transition is not well understood in discontinuous high boreal environments. In temperate peatlands climate warming has enabled re-emergence of forest due to landscape-wide dewatering (Jeglum and He Fangliang, 1995; Pellerin and Lavoie, 2000; Lohila et al., 2011), while similar trends have been observed within the Taiga Plains (Carpino et al. 2018; Chasmer & Hopkinson 2016). This study seeks to characterize the hydrological function of treed collapse-scar wetlands or 'treed bogs' as well as quantify both their extent and trajectory within Scotty Creek. This will be accomplished through the following specific objectives: 1) use geophysical methods to determine the presence or absence of ground ice or permafrost below treed bogs; 2) examine variations in snow cover

characteristics, depth of refreeze, soil moisture, and hydrostatic water level of treed bogs and adjacent treeless bogs and peat plateaux; 3) define the spatial extent of treed bogs within in a small area of interest based on their spectral and physical properties derived from remotely sensed datasets; and 4) present a conceptual model describing the formation, expansion and hydrological implication of treed bogs.

## 2.3 Study Site

Field studies were conducted at Scotty Creek Research Basin located 50km south of Fort Simpson, NWT located within the southern Taiga Plains ecozone (Figure 1). Scotty Creek is a 152km<sup>2</sup> basin and is typical to other watersheds in the lower Liard River Valley. The basin is underlain by discontinuous-sporadic permafrost (Quinton et al. 2011) (~40% coverage) and the headwaters are dominated by large peatland complexes, while the northern portion of the basin is dominated by mineral rich uplands intermixed with low elevation peatlands. The region has long, cold winters (average January temperature of -24.2°C) and short, warm summers (average July temperature of 17.4°C) with a mean annual air temperature (MAAT) of -3.2°C (MSC, 2019). In Scotty Creek, permafrost is typically restricted to forested peat plateaux, where the insulative properties of *Sphagnum spp.* produce the required thermal offset to sustain permafrost (Halsey et al. 1995). Permafrost in the basin is relatively warm and thin, with an average thickness between 5 and 10 m (McClymont et al. 2013). The permafrost bodies are interspersed by permafrost-free wetlands, which take the form of channel fens and collapse-scar bogs. Technically speaking, the entire peat plateau – wetland complex is classified as a bog (NWWG, 1988); the topographic depressions of the wetlands allow for internal drainage from the raised peat plateaux to the collapse-scar bogs, meaning that inputs into collapse-scar bogs are not strictly meteoric. Peat plateaux (43.0%), collapse-scar bogs (26.7%), channel fens (21.0%), and lakes (9.3%) are the four predominant landcover types within the headwaters of the basin (Quinton et al. 2011), each of which can be defined by their distinctive hydrological

roles and vegetation (Robinson & Moore 2000; Quinton et al. 2009). Peat plateaux are raised features (1 to 2 m) that contain woody vegetation with dense canopy coverage of *Picea mariana* (Halsey et al. 1995), often containing various herbaceous and lichen species (Vitt et al. 1994), and produce runoff into surrounding wetlands (Quinton et al. 2003). Collapse-scar bogs or “*treeless bogs*” are typically circular depressions within peat plateaux. The ground surface of collapse-scar bogs is typically about 1 m below the adjacent plateaux and these features are colonized by *Sphagnum spp.* mosses such as *S. riparium*, *S. fuscum*, and *S. angustifolium* (Robinson & Moore 2000). Collapse-scar bogs or “*Treeless bogs*” receive meteoric inputs, as well as lateral inputs from higher elevation peat plateaux. Because of this gradient, collapse-scar bogs are storage features within the plateau – wetland complex of the basin. Channel fens are geogenous features that receive water from both the surface and subsurface, and therefore, contain minerotrophic vegetation such as true mosses (bryophyta) and peat mosses (Vitt et al. 1994). Fens are linear features ranging between 50 – 100 m in width, and act as the primary method of water transport within the headwaters of the basin (Quinton et al. 2003). Treed collapse-scar bogs or “*Treed bogs*” are the same elevation as the surrounding collapse-scar features, and can be characterized by *S. fuscum* hummocks, ground lichen (*Cladonia spp.*), Labrador tea (*Rhododendron groenlandicum*), and sparse black spruce coverage (*Picea mariana*).

## **2.4 Methods**

### **2.4.1 Site selection**

A treed bog, surrounding collapse-scar bog, and peat plateau were selected based on visual inspection that occurred in September 2017. The criteria for the initial treed bog site selection included (1) examining for the presence of a black spruce canopy, and (2) evaluating whether the site could be considered low elevation. For this analysis, a treed bog site was considered low elevation if it was similar to that of an adjacent treeless bog. Site 1 was

investigated prior to installing instrumentation, and the treed bog at Site 1 was met the criteria described above. Treed bogs within Sites 2 – 4 were selected based on an initial landcover classification prior to physical investigation, while site selection for treeless bogs and peat plateaux was based on previous knowledge of these well studied landcover types. The initial site classification is described in detail in Appendix A. In total, four treed bogs sites were selected. Sites 1 and 2 contain a treed bog, an adjacent treeless bog, and a peat plateau, while Sites 2 and 4 are isolated within larger bog complexes and are not located near a stable plateau. Site 1 (Figure 1c) was the most intensively measured of all four study sites.

#### **2.4.2 Geophysical Investigation**

ERT measurements were completed at Site 1 only due to logistical constraints. Site 1 is a small connected treeless bog with an adjacent treed bog and peat plateau, and two geophysical transects were selected and ranged in length from 25 m to 183 m (Figure 1c). Transect (a) was 183 m long and was established to be spatially representative of all three landcover types, while transect (b) was 25 m long and was established near areas of denser canopy within the treed bog. ERT measurements are effective in permafrost environments due to differences in electrical resistivity between frozen and unfrozen materials (Kneisel et al. 2008). In an ERT survey, resistivity values are collected from transects of electrodes to produce a 2D-model of the subsurface. A Wenner electrode configuration was chosen to acquire ERT data (Kneisel 2006) due to the high-water content of peatlands and the relatively low current emitted from the electrodes in the survey. This array configuration combines reasonable vertical and horizontal resolution and has higher signal strength than other arrays, which may be required due to the high ice content and resistivity of the permafrost body. An electrode spacing of 1 m was used to ensure adequate vertical and horizontal accuracy, and differential GPS (dGPS; Leica Viva Series, GS10) measurements were collected at each electrode position to add vertical ground elevations in the final resistivity plot. An AGI SuperSting 8-channel ERT

system with 56 electrodes was used to collect resistivity data. After the resistivity values were collected, the data were processed using inversion software to produce a cross-section of the subsurface. *EarthImager 2D Inversion Software* was used to complete the conversion of resistivity data.

### **2.4.3 Snowpack Characteristics**

To determine how snowmelt varied between the three landcover types, snow survey transects were completed every 2 to 3 days between mid-March and the beginning of snowmelt, and every day during snowmelt to capture daily snowmelt. Snow depth was determined by inserting a metal ruler into the snowpack, and snow density was measured with a GeoScientific ESC-30 snow tube sampler (inner diameter of 30 cm). Because there is a greater variance in depth than density, depth measurements were taken every 5 m while density measurements were taken every 10 m. The transect was 175 m and was comprised of five density measurements in each landcover type at Site 1 and was selected to be representative of each landcover type studied here. The collected depth and density values were then used to compute SWE (snow water equivalent) throughout the melt period. Unfortunately, SWE measurements were stopped pre-maturely, thus linear interpolation was used to determine the snow depth and SWE for the remaining snowmelt period for each landcover type ( $\pm 1$  day).

Areal extent of snow cover represents the proportion of the landcover feature that is covered in snow at a given time. Unmanned aerial vehicle (UAV) flights were completed every day during snowmelt using a DJI Phantom 3 Professional, and images were mosaicked using Pix4D (Pix4D S.A., Switzerland) at a spatial resolution of 0.0348m. An iso-cluster unsupervised image classification was completed to distinguish between snow covered and snow free areas. Confusion matrices were computed for each day to test the accuracy of the unsupervised image classification using ArcGIS (Esri, Redlands, California). The SCA classification for each day was then overlain with the supervised image classification described below and was used to

determine the percentage (%) of snow cover for each landcover type over the duration of snowmelt (Figure 4) (For more information regarding the SCA image collection, refer to Appendix A).

#### **2.4.4 Seasonal ground freeze and thaw**

In order to assess the seasonal ground thaw of each landcover type, depth of refreeze and active layer measurements were completed immediately following snowmelt. If the active layer had not frozen to the underlying permafrost (*i.e.* presence of a talik), the thickness of the seasonally frozen layer was assumed to be the active layer thickness. If the ground experienced complete refreeze to the permafrost, active layer thickness was assumed to be the maximum depth of thaw as measured in August (Connon *et al.*, 2018). In each land cover type, this measurement will give insight towards how vegetation or soil moisture may impact the thermal regime of the subsurface. Measurements to determine the thickness of the seasonally frozen layer were completed by inserting a frost probe into the ground, and the process was repeated until the probe broke through the seasonal ground ice layer, at which point a measurement was taken and considered the depth of the seasonal ground ice layer. These measurements were taken along a total of four 25m transects through each landcover type, as well as along the geophysical transects at site 1 immediately following snowmelt. Rate of thaw was subsequently recorded at each point on a daily basis by measuring the depth from the ground surface to the top of the seasonally frozen layer. Ground temperature was measured using five temperature-moisture (TM) probes connected to data loggers (EM50, METER Environment, USA) were placed at five depths (5/10/15/20/25cm) in each landcover type at Site 1. Only the temperature data from 10 cm below the surface is presented here. The accuracy of the temperature measurements is  $\pm 1^{\circ}\text{C}$  (For more information regarding active layer measurements and ground temperature, refer to Appendix A).

### **2.4.5 Soil Moisture**

Discrete soil moisture measurements were collected at all four study sites using a handheld Hydrosense II (Campbell Scientific, Edmonton, AB) time domain reflectometry (TDR) metre. The Hydrosense II TDR provides a depth-integrated soil moisture measurement of the top 20 cm. A total of five soil moisture transects were selected through each landcover type. Measurements were taken at 5 m intervals along a 25 m transect through each land cover feature (Figure 1). At each measurement location, four measurements were taken in a radial direction and combined to calculate an average value of near-surface soil moisture. Twenty points were also taken within plateau features with a talik. Three temperature-moisture (TM) probes connected to data loggers (EM50, METER Environment, USA) were placed at five depths (5/10/15/20/25cm) in the upper soil horizon to capture continuous near surface variability in soil moisture throughout the summer at Site 1. One set of EM50s was installed in the plateau, one in the treeless bog, and one in the treed bog. The EM50 units measure and record soil moisture and ground temperature at 30-minute intervals. Both probes were calibrated according to the manual with samples of peat collected from Scotty Creek.

### **2.4.6 Water level fluctuations and hydrograph recession**

To examine differences in water table fluctuations, nine slotted 1.5 m PVC wells were instrumented with total pressure transducers (Hobo, U20) and were installed at all four study sites (Figure 1). The wells were perforated at 25 cm intervals down the entire length of the PVC and were installed by auguring and removing peat until the well could be installed at the desired depth (~ 1.25 m below the surface). A well was installed in each treed and treeless bog, as well as on a single plateau at Site 1 immediately following melt. Pressure measurements from each transducer were logged and recorded at 30-minute intervals on an internally contained data logger. Depth of the water table below the ground surface was determined by subtracting the average ground elevation measured in the spring by the water table elevation throughout the

time series. To support this calculation and determine water table depth, dGPS measurements were collected to obtain high-quality elevation and water table measurements at each well location ( $\pm 2\text{cm}$ ) (For more information regarding well installation and measurements, refer to Appendix A).

Recession analysis was completed to compare the rate of water table recession following precipitation events, and is commonly completed to characterize the recession of a stream hydrograph using the simple empirical relationship between discharge and time (Tallaksen 1995). Studies have also utilized it to characterize the recession of ground water within aquifers, as well as the water table recession in peatlands (Menberu et al. 2016; Bourgault et al. 2017). In this study, recession coefficients were determined using water table elevation and a simple exponential equation:

$$[1] \quad Q_t = Q_o e^{-at}$$

Where  $Q_t$  is water table elevation (masl) at time  $t$  after the start of the recession,  $Q_o$  is the water table elevation (masl) at the start of the recession,  $e$  is the natural logarithm,  $a$  is the recession coefficient ( $\text{day}^{-1}$ ) and  $t$  is time. Analysis of recession coefficients was evaluated for 5-days or up to the following precipitation event. To characterize how each site responds throughout the measurement period, the master recession curve (MRC) was determined using the same exponential relationship above. The MRC represents the compilation of multiple recession curves throughout the time series into a single curve that provides an average characterization of hydrological response (Posavec *et al.*, 2006). Because of this, the MRC represents the most probable recession under given scenario (Nathan & McMahon 1990; Posavec et al. 2006) (For more information regarding the recession analysis, refer to Appendix A). Rainfall was measured using a tipping bucket rain gauge at a nearby (500 m) meteorological station and was calibrated at 1 tip  $0.25 \text{ mm}^{-1}$ . The rain gauge was connected to a Campbell Scientific CR1000 datalogger and measured total tips over 30-minute intervals

#### **2.4.7 Image classification and analysis**

Remote sensing-based classifications landscape have been widely utilized for a variety of studies within discontinuous permafrost regions. Previous analysis have used the presence of a tree canopy as a proxy for determining the spatial extent of permafrost in Scotty Creek and other areas of low-relief discontinuous permafrost terrains (Chasmer et al. 2011; Quinton et al. 2011; Pastick et al. 2015). Due to the unique characteristics of treed bogs, canopy coverage may not always be an appropriate variable for determining permafrost extent. Although manual delineation is often a simpler approach, it would likely under-estimated permafrost distributions as it relied solely on canopy cover. Other basin-wide studies within Scotty Creek have used exclusively multi-spectral imagery to complete classifications (Quinton et al. 2003; Quinton et al. 2011), while a recent classification completed by Chasmer et al., 2014 utilized the integration of multi-spectral imagery and LiDAR derived products within Scotty Creek. In this analysis, a supervised image classification using WorldView-2 8-band imagery and an object-based analysis of LiDAR data was completed to determine the extent of treed bogs within a small AOI. The supervised image classification used a support vector machine (SVM) algorithm to determine the extent of treed bogs features. Twenty-five training sites were used for peat plateaux, fens and treeless bogs as these features are easily interpreted from aerial imagery. Only ten treed bog training sites could be selected as only a select few sites were verified as such in the field. Open water was masked out of the final imagery to reduce discrepancy within the classification. SVM was chosen as the classification method as it is less susceptible to correlated bands, as well as an unbalanced number or size of training sites. Because both the area and number of training sites were variable for each landcover type, this was the optimal classification technique. Once the supervised classification was completed, a low pass filter (3x3) and boundary clean tool were used to reduce noise and 'speckle' of the classified spectral product. To complete the topographic classification, LiDAR derived products (DEM, CHM, and canopy gap fraction) were used to classify each landcover type. Topographic position index

(TPI) as used to detrend the DEM and highlight topographically high ( $>0.100076$ ) and low ( $\leq 0.100076$ ) features. This method utilizes neighbourhood based focal statistics to determine the mean elevation within a specified area. A circular neighbourhood (125 m) was optimal as it best highlighted high and low elevation features. In terms of canopy height and gap fraction, thresholds were determined iteratively using a manual interpretation of the imagery and thresholds for all products used are summarized below (Appendix D). Once thresholds were established, the topographic and multi-spectral classifications were combined using a series of Boolean decisions (For more information regarding classification methods, refer to Appendix A). The final classification for each landcover type was then combined into the final classified raster (Figure 10). Classification accuracy was determined by using a confusion matrix on a per landcover basis with 250 assessment points distributed throughout the final classified raster, and Cohen's Kappa was used to determine how the classification performed in comparison to chance. The AOI for this analysis was selected as it is representative of the peatland landscape within the headwaters of the basin.

#### **2.4.8 Statistical Analyses**

Comparison of mean SWE, thickness of the seasonally frozen layer, and recession slope between each landcover type in this study was achieved using a one-way analysis of variance test (Appendix C). Because there was not a common variance amongst thickness of the seasonally frozen layer data, a Welch one-sided test was used due to the relaxed common variance assumption. Data was tested for normality using a Shapiro-Wilks test. A logarithmic transformation had to be completed on SWE data to ensure a normal distribution. All statistical tests were completed using the R statistical environment (R core development team, version 3.5.2). Level of significance ( $\alpha$ ) for statistical comparisons was set to  $\alpha < 0.05$ .

## 2.5 Results and discussion

### 2.5.1 Geophysical Investigation

The electrical resistivities measured in the upper 50 cm of the treed and treeless bog portion of Transect 1 are indicative of drier peat, while the higher resistivities ( $>500\Omega\text{m}$ ) within the upper 50 cm of the peat plateau are due to the high ice content of the active layer (Figure 2). Variations in resistivity within the active layer are easily interpreted due to the stark transition between the low resistivities of the thawed active layer and high resistivities of the permafrost body. There are non-substantial differences between treeless bogs and treed bogs below 1m, and the resistivities found below this depth ( $<100\Omega\text{m}$ ) are generally consistent with permafrost free conditions composed of unfrozen peat and clay-rich till deposits. The peat substrate transitions to clay mineral soil at approximately 2.5 to 3.0 m below the surface. Resistivities of  $>5000\Omega\text{m}$  approximately 50 cm below the ground surface of the peat plateau are interpreted as permafrost, which is consistent with frost probe measurements. ERT Transect 2 (Figure 2) is shorter in length (28 m) and was measured in August 2018. This transect measured to a depth of approximately 4 m below the ground surface. Again, low resistivities below 1 m were interpreted as permafrost free conditions, whereas the low resistivities at the start of this transect are consistent with drier surface peats (Lewkowicz et al. 2011). The high resistivities near the end of Transect 2 (between electrodes 22 and 28) are indicative of pore ice, which suggest the presence of ice bulbs beneath the surface. Observations with a frost probe indicated that this ice was on average 58 cm below the surface and on average 11 cm thick ( $n=8$ ). As these measurements were taken in late August 2018, it is likely that this ice persisted throughout the entire summer period.

These results indicate that treed bogs are free of permafrost with no notable differences between the subsurface stratigraphy between treed and treeless bogs. Previous geophysical investigations completed within Scotty Creek (McClymont et al. 2013), and in other regions of

discontinuous permafrost (Lewkowicz et al. 2011) found similar resistivities within collapse-scar bogs and peat plateaux. McClymont et al. (2013) noted high resistivities ( $> 5000 \Omega\text{m}$ ) beneath the ground surface of peat plateaux within Scotty Creek, which is consistent with the resistivities measured within the peat plateaux at Transect 1. The same study by McClymont et al. (2013) notes low resistivities ( $<100 \Omega\text{m}$ ) both below the permafrost body and within open bogs, which are consistent with saturated peat and mineral soil substrates. Lewkowicz et al. (2011) found that permafrost bodies within sporadic-discontinuous peatland sites had resistivities  $\sim 2000 \Omega\text{m}$  due to potential high unfrozen water content, while permafrost-free organic layers had very low resistivities.

### **2.5.2 Snowpack Characteristics**

All three features gain and lose SWE differently due to variability in land cover characteristics such as canopy cover and hummocky terrain. Plateaux had the highest SWE ( $117 \text{ mm} \pm 18 \text{ mm}$ ) and snowpack depth ( $65 \text{ cm} \pm 5 \text{ cm}$ ), while the treeless collapse-scar bogs had the lowest SWE ( $97 \text{ mm} \pm 11 \text{ mm}$ ) and snowpack depth ( $57 \text{ cm} \pm 5 \text{ cm}$ ). This difference was not significant ( $p = 0.06$ ). Both the SWE ( $105 \text{ mm} \pm 10 \text{ mm}$ ) and snowpack depth ( $59 \text{ cm} \pm 7 \text{ cm}$ ) of treed bogs was in between treeless bogs and peat plateaux, but there was not a statistically significant difference between treed bogs and any other landcover type ( $p > 0.05$ ). In forested regions, land cover properties strongly influence snow accumulation. For example, peat plateaux support sparse forest stands and therefore support deeper snow packs compared to treeless bogs (Figure 3), as open areas are more susceptible to both redistribution and wind-blown sublimation (Golding & Swanson 1986; Pomeroy et al. 2002). In a dense stand of boreal black spruce (*Picea mariana*) trees, snow accumulation is typically lower beneath the canopy (Pomeroy et al. 2002), but this effect is dependent on the effective Leaf Area Index (LAI) of the canopy. At Scotty Creek, the LAI of the black spruce canopy cover is lower than the LAI of black spruce reported by studies in other cold regions (Pomeroy et al. 2002) (For more information

regarding SWE accumulation and LAI, refer to Appendix B), resulting in higher accumulation compared to open areas. Previous studies conducted at Scotty Creek found similar trends, where the lowest SWE values were found in treeless bogs and the highest within peat plateaux (Haughton 2018). The snowpack within treed bogs is intermediary between treeless bogs and peat plateaux and the sparse canopy cover within these features may prevent the redistribution and sublimation observed in areas that are lacking canopy cover, while still allowing interception to occur in pockets of more densely packed canopy.

At the beginning of the April, the peat plateaux consistently had the highest SWE, while treeless bogs had the lowest. When melt intensifies ( $>5 \text{ mm day}^{-1}$ ), treeless bogs experience the most rapid volumetric loss in SWE, while treed bogs and peat plateaux experience similar losses. At the end of the measurement period, treed bogs ( $86 \text{ mm} \pm 29 \text{ mm}$ ) retained the greatest SWE, while treeless bogs had the least ( $70 \text{ mm} \pm 21 \text{ mm}$ ) (Figure 3). Once again, there was no statistical difference between any of the landcover types ( $p > 0.05$ ). After 26-April, SWE was computed using a linear interpolation and a similar trend emerges such that melt occurs more quickly in open area's (i.e. treeless bogs) and less quickly in treed landscapes (i.e. treed bogs and peat plateaux). The areal loss of snow cover was also more rapid in treeless bogs compared treed bogs and peat plateaux (Figure 3). Early in the analysis, peat plateaux had the largest SCA (90%), followed by treed bogs (87%) and treeless bogs (86%). By the end of the SCA measurements, approximately 33% of peat plateaux ground surfaces were still covered by snow, while treed bogs were 17% snow covered, and treeless bogs just 3% snow covered. The overall accuracy of the classification on 25-Apr was 88% (Kappa = 0.76) and increased to 98% for the remaining classified images (Appendix E). A detailed breakdown of the accuracy assessment is included in Appendix B.

During snowmelt, long and shortwave radiation and turbulent fluxes strongly influence the rate at which the loss of snowpack occurs (Sicart et al. 2004). In open areas (i.e. treeless

bogs) there is an increase in solar radiation, a greater loss of long-wave radiation, as well as increased contributions from turbulent fluxes due to lack of canopy cover (Marks et al. 1998), and because of this, open areas have an earlier onset of snowmelt relative to treed areas (Harding & Pomeroy 1996; Davis et al. 1997). When canopy cover is present, there is a reduction in both the turbulent and radiative fluxes that may contribute to snowmelt and a resultant decrease in the snowmelt rate (Sicart et al. 2004). These trends have been widely observed throughout Scotty Creek (Haughton 2018; Quinton et al. 2019), as well as in similar environments throughout northern regions (Sicart et al. 2004; Hardy et al. 2004). At Scotty Creek, snowmelt is driven by incoming shortwave radiation such that melt rates in treeless landscapes occurs earlier and quicker than in treed areas. (Haughton 2018; Quinton et al. 2019), where turbulent fluxes contribute between 12% and 32% of energy available for melt, and 70% to 80% of net radiation is available for melt energy. Although four component radiation was not measured, stable plateaux typically receive 80% of the total incoming shortwave radiation that is received by a treeless bog (Connon et al. 2018). The increase in incoming shortwave radiation due to canopy thinning on an unstable plateaux (Connon et al. 2018; Chasmer et al. 2011) may provide an estimate of the interactions between canopy cover and incoming shortwave radiation within treed bogs. The intermediate depletion of the snowpack of treed bogs is likely due to variable amounts of shortwave radiation and sublimation compared to peat plateaux and treeless bogs due to the presence of a sparse canopy within these landcover types.

### **2.5.3 Seasonal ground freeze and thaw**

Plateaux with taliks or “unstable plateau” have the greatest average depth of refreeze (60 cm ± 10 cm) (Figure 5). There was a statistically significant ( $p < 0.05$ ) difference in re-freeze depths between treeless bogs (38 cm ± 7 cm) and both other land cover types, while there was not a significant difference between treed bogs (56 cm ± 13 cm) and plateaux (60 cm ± 10 cm).

Furthermore, the winter ground temperatures (10 cm below the surface) of treed bogs and peat plateaux were similar (Figure 6). The ground temperatures at 10 cm depth within the treeless bog at Site 1 remained isothermal (just below 0°C) for the entire winter, while both treed bogs and peat plateaux are frozen for most of the winter. The treeless bog remained just below freezing at 10 cm depth for the entire winter, while the peat plateau was the quickest to freeze (~2-weeks), and treed bogs dropped below the isothermal period after approximately three months. Thaw rates among landcover features also varied. For example, treeless bogs thawed the quickest, losing their ground ice within 1-3 weeks of snowmelt, while ground ice within the treed bogs persisted much longer throughout the summer, with six of the twenty measurement points retaining ice for the entire summer.

Despite treed bogs being devoid of permafrost, the thermal and hydrological conditions allow the freezing front to penetrate to a depth similar to that of an unstable plateau, creating a mechanism for potential inter-annual ice bulbs. The variation in ground temperatures between treed and treeless bogs suggests significant variations in both the subsurface and heat conduction properties of treed bogs. For example, soil moisture exerts a strong control on the thermal properties of peatlands (Atchley et al. 2016), as the high porosity of peat allows for large seasonal and annual changes in volumetric water content. The depth integrated soil moisture of the treed bog was lower than that of the treeless bog site, which lowers the amount of energy loss needed to freeze the substrate. The peat plateau was the driest of the three land cover types at 10 cm depth, and therefore was the quickest to freeze. The ground ice within treed bogs also persisted much longer throughout the spring and summer compared to treeless bogs. The extended thaw period within treed bogs is likely due to both the larger depths of refreeze and the subsequently higher energy requirements needed to completely thaw the substrate. In terms of peat plateaux, SWE and lower soil moisture are hypothesized to result in larger depths of refreeze compared to other landcover types in this study. As plateaux become unstable, the

active layer may not refreeze entirely to the frost table, resulting in the formation of a supra-permafrost talik. A recent model produced by Devoie et al. (2019) demonstrated that soil moisture, SWE, ground heat flux, and timing of snowfall play the largest roles in talik formation and reduced refreeze depths within unstable peat plateaux at Scotty Creek. The larger refreeze depths within treed bogs may be impacted similarly, such that lower soil moisture values, ground heat flux, and denser canopies result in larger refreeze depths compared to treeless bogs.

#### **2.5.4 Soil Moisture**

Discrete soil moisture measurements varied amongst all land cover features immediately following snowmelt. Unstable plateaux (with a talik) had a depth integrated VWC of  $58\% \pm 4\%$ , whereas treed bogs had a lower VWC average of  $38\% \pm 4\%$ . The driest conditions were found in peat plateaux not exhibiting thaw, with an average VWC of  $30\% \pm 4\%$ , while treeless bogs were the most saturated with an average VWC of  $68\% \pm 2\%$ . Over the measurement period, the VWC of treeless bog was consistently above 60%, while peat plateaux were consistently the driest of the landcovers (Appendix F). Treed bogs were in-between peat plateaux and treeless bogs, supporting the hypothesis that soil moisture differences exist between these landcover types, while unstable plateaux had a higher VWC than treed bogs throughout the measurement period (Appendix F). At Site 1, where soil moisture was continuously monitored, the most saturated conditions were present within the treeless bog and the driest conditions were recorded within the peat plateau (Figure 7). Treed bogs were consistently more saturated than plateaux, but less saturated than treeless bogs at all measurement depths. For example, treeless bogs are completely saturated at 15 cm below the ground surface, while treed bogs did not become saturated until 25 cm below the surface. Peat plateaux remained driest throughout the entire summer, and only experience higher levels of saturation in the lower 25 cm where further infiltration is limited by the frost table.

The soil moisture conditions present within each land cover type will be indicative of its approximate hydrological role. Collapse-scar wetlands act as depressional storage features (Beilman et al., 2001), and therefore, it is expected that they have the highest integrated VWC due to the water table often being at or near the surface (Figure 7). Due to the elevation gradient between plateaux and lower elevation features, peat plateaux are often well drained features with a distinctly low near-surface VWC (Figure 7). Talik development within peat plateaux can dramatically alter its hydrological regime and may result in a higher VWC due to a decrease in the elevational gradient and subsequent pooling of runoff (Connon et al. 2018). In terms of treed bogs, several studies have noted increased rates of peat accumulation and net vertical growth of collapse-scar wetlands within the boreal peatlands (Robinson & Moore 2000; Turetsky et al. 2000; Camill et al. 2001; Turetsky et al. 2007). Although soil moisture conditions appear to be drier within treed bogs, the lower volumetric values may be a product of this vertical growth above the water table, as both treeless and treed bogs remain completely saturated for 2 – 3 m below the surface. Therefore, the slight elevational difference of the surface above the water table within may provide the drier surface conditions and may be ideal for the growth of drier vegetation communities such as hummocky *Sphagnum spp.* and black spruce trees (Camill 1999; Vitt et al. 1994; Beilman 2001).

### **2.5.5 Water level fluctuations and hydrograph recession**

At each well location, the elevation of the water table was higher within treed bogs compared to treeless bogs (Figure 8). The peat plateau had the highest water table elevation and is also elevated above adjacent lower elevation landcover types (i.e. collapse-scar treed and treeless bogs, fens), and because of this, lower elevation landcover receive runoff due to the stark hydraulic gradients.(Wright et al. 2008; Hayashi et al. 2004). The elevated water tables within treed bogs may result in a small hydraulic gradient to lower elevation treeless bogs, as the perched water table and higher ground elevation is indicative of their presence within the

peatland portion of this basin (Wright et al. 2008), however, the gradients could not be quantified in this study. The water table positions were also deeper below the ground surface in treed bogs and closer to the surface in treeless bogs (Figure 8).

The single peat plateau well had the largest recession coefficient (Figure 9), which is expected as these features act as runoff generators within the peatland portion of the basin (Wright et al. 2009) due to their larger hydraulic gradients. Treeless bogs experienced the smallest recession coefficient of all three landcover types, whereas the water table recession within treed bogs was higher. The difference in recession coefficients between treed and treeless bogs was statistically significant ( $p < 0.05$ ). The peat plateau well was excluded from the statistical analysis due to its small sample size ( $n=1$ ), but the mean recession coefficient was an order of magnitude larger compared to treed and treeless bogs (Figure 9). The MRC's for treed bog sites were steeper and shorter compared to treeless bogs, indicating that water table recession within treed bogs are generally both shorter and more rapid. However, it should be noted that the MRC of the treeless bog at Site 4 was more rapid than the adjacent treed bog, which indicates potential variability in the water table response of treed bog sites.

The more rapid water table recession of treed bogs compared to treeless bogs could be a result of multiple mechanisms. Specific yield strongly influences the response of the water table within peatlands, and represents the ratio of volume of water that is yielded by gravity drainage by the volume of the block of soil (Price et al. 2003). In peatlands, a high specific yield is typically found in the upper horizons of peat (i.e. acrotelm peat) where pore space is high and it can be more easily drained by gravity; whereas low specific yield is often observed in the lower horizons of decomposing peat (i.e. catotelm peat) where pore space is smaller (Price et al. 2003). If the water table is within the catotelm, it will respond more rapidly to inputs and recede more quickly, and if the opposite is true, the water table response will be muted and recessions will be slower (Price et al. 2003). At Scotty Creek, the specific yield of the peat

substrate decreases with depth, as the pore space within decomposed peat layers are smaller (Quinton & Gray 2003). Although specific yield was not measured for this study, the larger mean water table recession within treed bogs suggests possible variation in specific yield, as the water table is lower below the surface and may reside in more decomposed peat.

Evapotranspiration (ET) can also influence the recession of the water table, as it represents one of the most significant energy fluxes in peatlands (Wu et al. 2010; Lafleur et al. 2005; Waddington et al. 2015). Although ET was not directly measured here, ET contributions from black spruce at Scotty Creek are generally poor (Warren et al. 2018), and it is unlikely that ET caused additional water table drawn down due to extremely poor transpiration rates (For more information regarding ET in permafrost peatlands, refer to Appendix B). However, possible relationships between water table recession and specific yield should be explored further, as it provides a possible distinction between the treed and treeless bogs due to lower water table position and more rapid recession within treed bogs.

### **2.5.6 Image classification and analysis**

A supervised image classification was completed using Worldview-2 and LiDAR imagery within the peatland portion of Scotty Creek. Peat plateaux covered 40% of the 16.8 km<sup>2</sup> classified area, and fens represent 32%, treeless bogs 12%, treed bogs 12%, and uplands 4% (Figure 10). It should be noted that open water was not classified in the final product. The overall accuracy of this classification was 85.3% (Kappa = 0.79) (Appendix F), and therefore misclassifications were limited to 14.7% (A detailed breakdown of the accuracy assessment is included in Appendix B). An early classification by Quinton et al. (2011) utilized manual delineation based on visual representation of canopy cover as a proxy for permafrost distributions within a smaller portion of the larger AOI selected in this study (1.0 km<sup>2</sup>). The authors reported that peat plateaux represent 43.0% of the classified area, while collapse-scar bogs and channel fens represented 26.7% and 21.0% respectively. As their classification only

accounted for canopy cover, it is likely that the classification over-estimated the area occupied by plateau as a portion of this landscape would have been treed but permafrost free. Although the authors did not quantify accuracy or error rate, previous studies using manual delineation have noted accuracies ranging between 40% and 70% (Chasmer et al. 2014). An updated classification of the basin using a combination of Worldview-2 multi-spectral imagery and LiDAR determined that uplands represented 48% of the basin, followed by peat plateaux (20%), bogs (19%), fens (12%) and lakes (2%) (Chasmer et al. 2014). The overall accuracy of this classification was 91% and averaged ~88% for each landcover type. Although the classification methodologies were similar to this study, there were discrepancies between the two classifications. The relative proportions of landscapes within the respective AOIs and the introduction of a new landcover type may ultimately lead to the discrepancies. The AOI presented here was more similar to the study area used by Quinton et al. (2011), as it focused on peatlands near the headwaters of the basin, and therefore there were more similar landcover proportions. Nevertheless, the classification completed in this study determined that treed bogs are a relatively widespread feature within the peatland portion of the basin.

### **2.5.7 Conceptual model of landscape succession**

Various characteristics differentiate treed and treeless bogs. For example, treed bogs accumulate deeper snowpack's, have greater depth of seasonal frost, and demonstrate differences in moisture retention and hydrological response properties. The differences between these two landcover types also encompass ecological factors such as tree density, species, and age (Haynes et al., *in prep*). Many studies have noted the widescale expansion of collapse-scar wetlands following rapid permafrost thaw within the Taiga Plains (Robinson & Moore 2000; Quinton et al. 2011; Baltzer et al. 2014; Zoltai 1993), while also hypothesizing on the impacts of such changes on the cycling of water and energy (Shur & Jorgenson 2007; Quinton et al. 2011; Helbig et al. 2016). A recent study completed by Helbig et al. (2016) hypothesized that

widescale forest loss and wetland expansion may lead to a net cooling effect due to increased albedo in the winter and increased ET in the summer. Similarly, Haughton et al. (2018) noted wetland expansion would lead to a delayed but rapid onset of snowmelt, resulting in a decreased lag time and a flashier hydrograph at the basin outlet. The gradual de-watering of peatlands, increasing productivity, and canopy re-establishment are a less established and emergent trend in discontinuous permafrost peatlands (Kettridge et al. 2013; Baltzer et al. 2014; Chasmer & Hopkins 2016). For example, a notable decrease in water levels of hydrologically connected collapse-scar wetlands within Scotty Creek occurred over a 14-year period, (Haynes et al. 2018), while forest expansions has been observed in southern regions of the Taiga Plains where permafrost thaw had already advanced (Carpino et al. 2018). More importantly, remote sensing analysis within Scotty Creek noted minor increases in woody vegetation/shrub growth within locally elevated wetlands (Chasmer & Hopkins 2016).

The conceptual diagram presented here (Figure 11) outlines the observed differences in snow cover, ground ice, canopy cover, ground elevation, and water table between the three distinct landcover types in this analysis, as well as outlines the trajectory of post-thaw landscapes and the formation of treed bogs. Here it is proposed that both spatial and temporal transitions will eventually lead to re-establishment of canopy cover within previously treeless permafrost-free landscapes within the Southern Taiga Plains. In the winter and early spring, treed bogs accumulated a deeper snowpack and had lower melt rates as they maintained their snowpack longer than treeless bogs. During the same period, peat plateaux had the largest snowpack and longest melt period (Figure 3). This difference in melt rate is likely due to the interception of short-wave radiation as there is sporadic canopy cover within treed bogs. Because of this, it is unlikely that melt will occur as rapidly as proposed by Haughton et al. (2018), but instead will occur gradually leading potential increases in lag time as well as a more muted basin hydrograph. However, the impact of the deeper and longer-lasting seasonal ice

observed in the late spring within treed bogs may direct freshet to the basin outlet more rapidly than in situations where treeless bogs are dominant. Similarly, canopy re-establishment within permafrost-free landscapes will eventually lead to a reduction in albedo similar to that of an unstable treed peat plateaux, which may impact the hypothesized increases in albedo and associated regional cooling following widescale wetland expansion noted by Helbig et al. 2016.

As the water table was deeper below the surface in treed bogs throughout the summer, the near surface soil moisture of the treed bog sites was lower than treeless bogs (Figure 7). Overtime, it would be plausible to estimate that continued landscape-wide dewatering (Haynes et al. 2018) and the upward growth of hummock forming species (Camill 1999) will continue to lower near surface soil moisture conditions throughout the summer, resulting in drier conditions that may further promote canopy re-establishment. However, soil moisture values may initially increase following permafrost thaw due to ground subsidence and inundation. Vegetation, depth of snow, and antecedent soil moisture all impact the thermal gradient that drives heat extraction and subsequent downward movement of the freezing front in the winter. This upward growth combined with the insulative properties of peat and drier surfaces may create conditions ideal for the larger depths of refreeze observed in this study (Figure 5). However, in the current climate it is unlikely that multi-year ice will develop below hummocks, although in some cases (and as demonstrated in this study and by Vitt et al. 1994), ice may persist for an entire summer. In terms of energy transfer, ET will likely increase following the expansion of treeless wetlands due to higher transpiration rates of *Sphagnum spp.* bogs (Warren et al. 2018; Helbig et al. 2016). However, a transition from treeless to treed wetlands may result in a subsequent reduction in ET, as contributions from black spruce within Scotty Creek are generally poor due to nutrient poor conditions (Warren et al. 2018; Baltzer et al. 2014). For example, Warren et al. (2018) found lower ET rates within peat plateaux compared to *Sphagnum spp.* dominated open bogs. Vascular vegetation may also reduce rates of ET as canopies shelter the surface from

turbulence and reduce the amount of radiation reaching the surface (Lafleur, 2008). Therefore, such a spatial transition may reduce ET rates in the long-term in regions like Scotty Creek.

Although the formation of treed bogs remains largely unknown, it is hypothesized that treed bogs are at a stage in the biophysical succession of collapse-scar wetlands, such that under a cooler climate the same processes would lead to the development of raised peat plateaux. However, the length of the transitional period from a treed permafrost-free landscape to treed permafrost landscape is vast. For example, Zoltai (1993) determined that permafrost free landscapes have taken upwards of 600 years to regenerate permafrost following a large-scale disturbance, while Camill (1999) found that the succession of *Sphagnum spp.* can lead to canopy re-establishment in a period as short as 50 to 80 years. It is assumed that the large disparity in time scales is due to the wide-scale canopy cover required for permafrost regeneration (Camill 1999). Currently, it is unclear as to whether landscape-wide dewatering or *Sphagnum spp.* succession will occur more quickly in Taiga Plains region, but a notable level of landscape dewatering was observed within a 14-year period at Scotty Creek (Haynes et al. 2018), while *Sphagnum spp.* succession can take much longer following permafrost thaw (Camill 1999). As the treeless bog landscapes continue to age, the growth of treed bogs within their center lawns is a plausible trajectory and would have significant implications for future water resources in the discontinuous permafrost zone of the Taiga Plains. Here, it is proposed that upward growth combined with the observed landscape wide dewatering will allow for canopy re-establishment and the subsequent development of treed bogs.

## **2.6 Conclusion**

This study improves the understanding of treed wetland landscapes within the peatland-dominated zone of discontinuous permafrost. Here it is demonstrated that treed bogs are permafrost-free and represent a new landcover type that appear to have evolved from a previously treeless collapse-scar bog but have not yet developed mature black spruce canopies.

The snow depth, soil moisture, and thickness of the seasonally frozen layer of treed bogs intersected both treeless bogs and peat plateaux, and a difference in water table elevation may result in hydraulic gradients between treed and treeless bog sites. There was also a notable difference in both the water table elevation and recession of treed and treeless bogs, suggesting either differences in the specific yield due to different water table positions, or differences in energy transfer. Because of these findings, it is proposed that treed bogs become a recognized landcover type within the discontinuous permafrost zone of the Taiga Plains. Future work should seek to gain a better understanding of the historical significance of treed bogs on the landscape, as well as understanding the trajectory of these features under a warming climate.

## **2.7 Acknowledgements**

We would like to thank the Dehcho First Nations, including the Liidlii Kue First Nation, Jean-Marie River First Nation and Sambaa K'e First Nation, for their support and acknowledge that the Scotty Creek Research Station is located on Treaty 11 land. We acknowledge funding support from a Natural Sciences and Engineering Research Council of Canada (NSERC) Discovery Grant. The 2010 Light Detection and Ranging (LiDAR) data and derived products (CHM, Canopy gap fraction) were provided by L. Chasmer and C. Hopkinson, University of Lethbridge.

## CHAPTER 3.0: Conclusion and future research

### 3.1 Summary and Conclusions

Rapid climate warming in northern Canada is leading to accelerated permafrost thaw and resultant landscape change. Because of this, it is increasingly important to understand how these landscapes are changing under warming conditions. Within the discontinuous permafrost zone, canopy cover was historically used as a proxy for determining permafrost extent (Quinton et al. 2011; Baltzer et al. 2014; Chasmer et al. 2010; Thie 1974), as it was hypothesized that a black spruce canopy could only persist atop raised peat plateaux. Rapid permafrost thaw often results in ground subsidence, inundation of the peat surface, and removal of the canopy due to saturation of the rooting network (Robinson & Moore 2000; Baltzer et al. 2014). Although these are well documented processes within the discontinuous permafrost zone, they did not appear to apply to treed bogs as these features are characterized by a sparse black spruce canopy, ground lichen, *Sphagnum* hummocks, and are low elevation. Previous studies have focused on understanding rapid canopy loss and permafrost thaw (Payette et al. 2004; Camill 2005; Baltzer et al. 2014), but few have examined how landscapes within the discontinuous zone are spatially and temporally transitioning under a warming climate. This research sought to provide an initial understanding on treed bogs in the context of discontinuous permafrost peatlands.

Prior to this analysis, permafrost presence beneath treed bogs was unclear. Geophysical investigations have been widely adopted to complete permafrost investigations in a wide variety of environments such as peatlands and continuous permafrost environments (Lewkowicz et al. 2011; McClymont et al. 2013; Kneisel 2006; Kneisel et al. 2008). In this study, high quality ERT data was used to determine that treed bogs are permafrost free features, and the resistivities found beneath treed bogs and treeless bogs were similar. Given that these features are treed

but are permafrost free, this research sought to understand how their physical characteristics differ from treeless bogs and peat plateaux. For example, variables such as snowpack characteristics, depth of seasonal frost, ground temperature, and soil moisture were examined, and were found to vary between treeless and treed bogs. Interestingly, the depth of seasonal frost and the ground temperatures of treed bogs was similar to that of an unstable plateau, indicating similarities in heat conduction properties. This research also examined water table fluctuations and recession, and once again, that water table recession was generally quicker in treed compared to treeless bogs, and it determined that observed differences in water table elevation between treed and treeless bogs that may result in a series of hydraulic gradients. Variations in specific yield at different water table positions between landcover types represents the most plausible explanation for the observed differences in the recession coefficients.

Finally, this research hypothesized on the formation of treed bogs within the discontinuous permafrost zone and provide and estimate for how widespread these features are throughout the headwaters of Scotty Creek. Early work that focused on peatland succession (Vitt et al. 1994; Zoltai 1993; Camill 1999) was used as a framework for presenting the formation of permafrost free treed bogs within this environment, such that the succession of *Sphagnum*, the establishment of black spruce, and the dewatering of these landscapes may provide the ideal conditions for the formation of treed bogs. This research also examined how widespread treed bogs are throughout the small AOI in the headwaters of the basin and determine that treed bogs represent a greater portion of the landscape than treeless bogs. This study focused on examining and characterising a previously unrecognized landcover type within the peatland portion of the southern discontinuous permafrost zone, and because of this analysis, it is proposed that treed bogs be recognized as their own landcover type within the discontinuous permafrost zone.

### 3.2 Future Research

This study sought to gain a better understanding of treed low elevation features within the discontinuous permafrost zone. Despite this, there are still many unanswered questions surrounding treed bogs on this landscape. For example, it was hypothesized that the formation of treed bogs occurred due to a combination of; (i) the successional processes of *Sphagnum* dominated peatlands, and (ii) the dewatering of the peatland portion of the basin. Nonetheless, the origin of treed bogs within this landscape is still largely unknown and would represent a significant step in understanding their true importance on the landscape. Reconstructing the history of these features would not only provide insights on their formation but would also provide insight into their permanence as a landcover type. Although there was no permafrost found beneath any of the treed bogs in this study, altered thaw processes occurring within an existing peat plateau may be an alternative hypothesis leading the formation of treed bogs, such that canopy cover persisted after thaw had occurred. Several questions remained unanswered regarding the current impact of treed bogs on the landscape. Although this paper examined differences between hydrological variables such as soil moisture and recession coefficients between landcover types, it did not examine how energy transfer influenced these variables throughout time. For example, evapotranspiration is one of the most significant energy fluxes within northern peatlands, and because of this, the impact of canopy cover within a treed bog on energy transfer should be examined. Other variables such as canopy health and persistence should also be explored, as the health, age, and productivity of the canopy cover remains suspect. Finally, just as the formation of these features is important, the permanence and trajectory of treed bogs on the landscape also remains unknown. This research determined that treed bogs are widespread throughout the headwaters of Scotty Creek, but future research should focus on gaining a more thorough understanding of how these landscapes continue to evolve under a rapidly warming climate, and should specifically examine the role treed bogs

play in future landscapes under a warming climate. This will provide a significant insight into the future of post-thaw landscapes within the discontinuous permafrost zone of the Taiga Plains.

# Figures

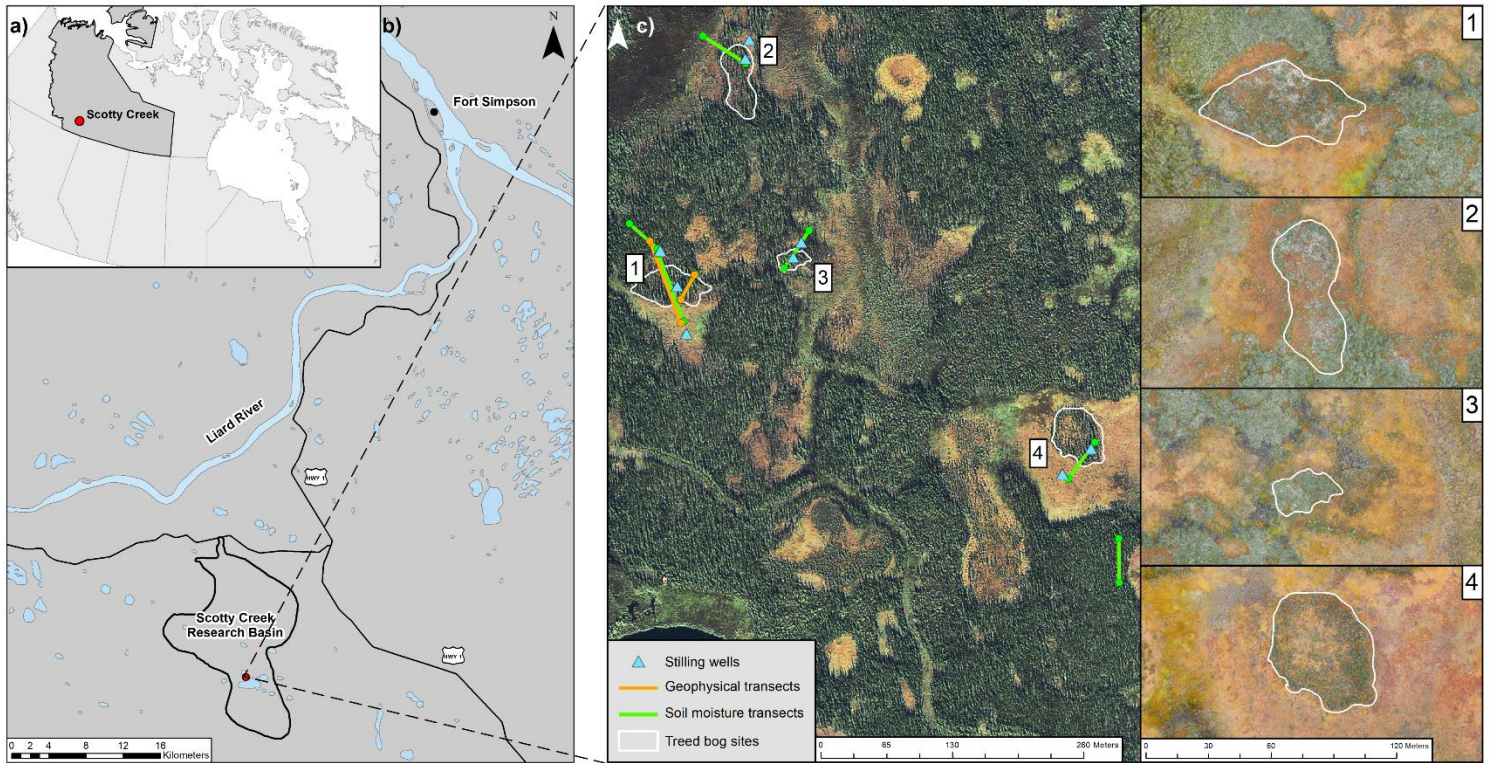
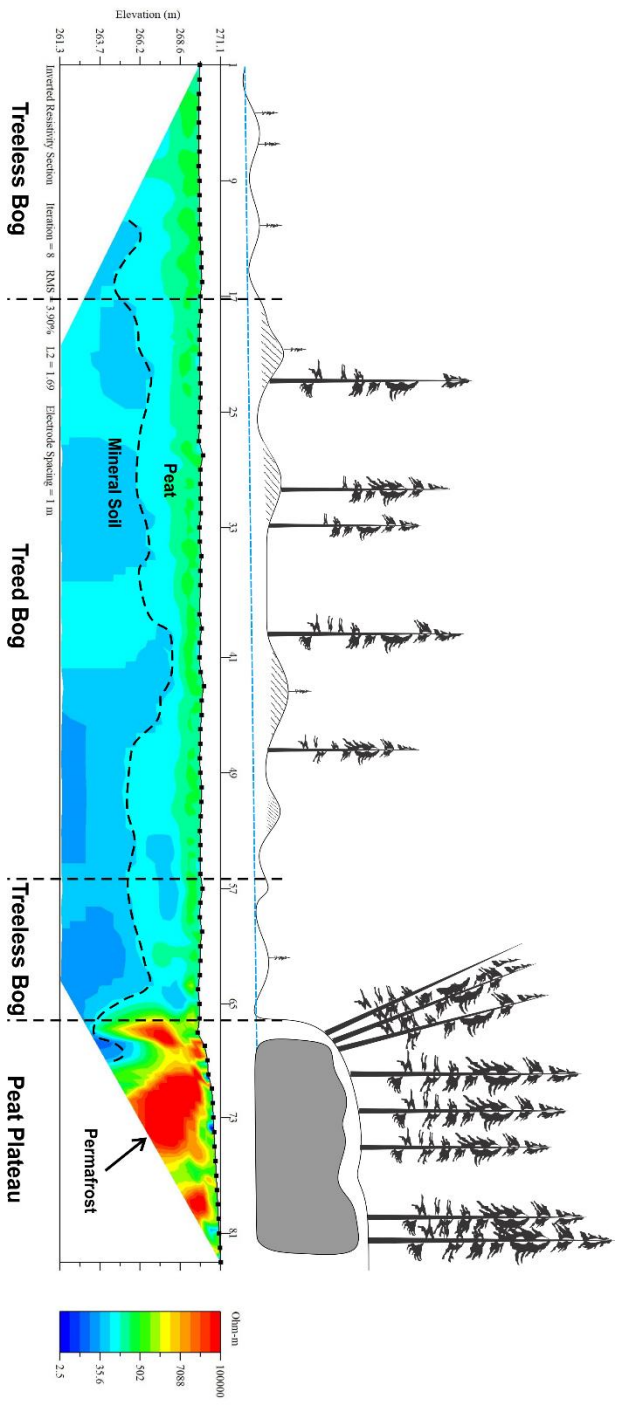


**Figure 1:** (a) Location of Scotty Creek, located 50km south of Fort Simpson, NWT. (b) Aerial imagery (Worldview-2) with each geophysical transect, soil moisture transects, and well locations plotted at each study site. (c) Each tree bog feature (sites 1-4) highlighted with high-quality ortho-mosaic imagery.

(a)



(b)

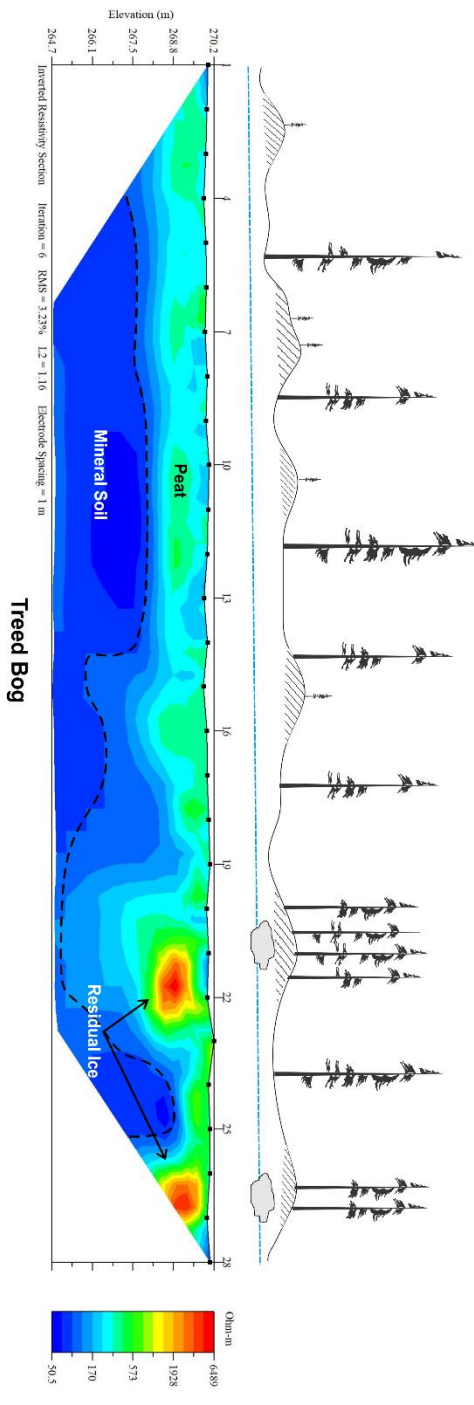


**Figure 2:** Electrical Resistivity Tomography (ERT) transects for site 1. (a) Transect 1 (83m) includes all three landcover types. (b) Transect 2 (28m) measures Treed bog. Note difference in scale between the two plots. Representation of vegetation on each transect is an illustration of approximate vegetation differences among landcover types. Measurements were completed in August 2018

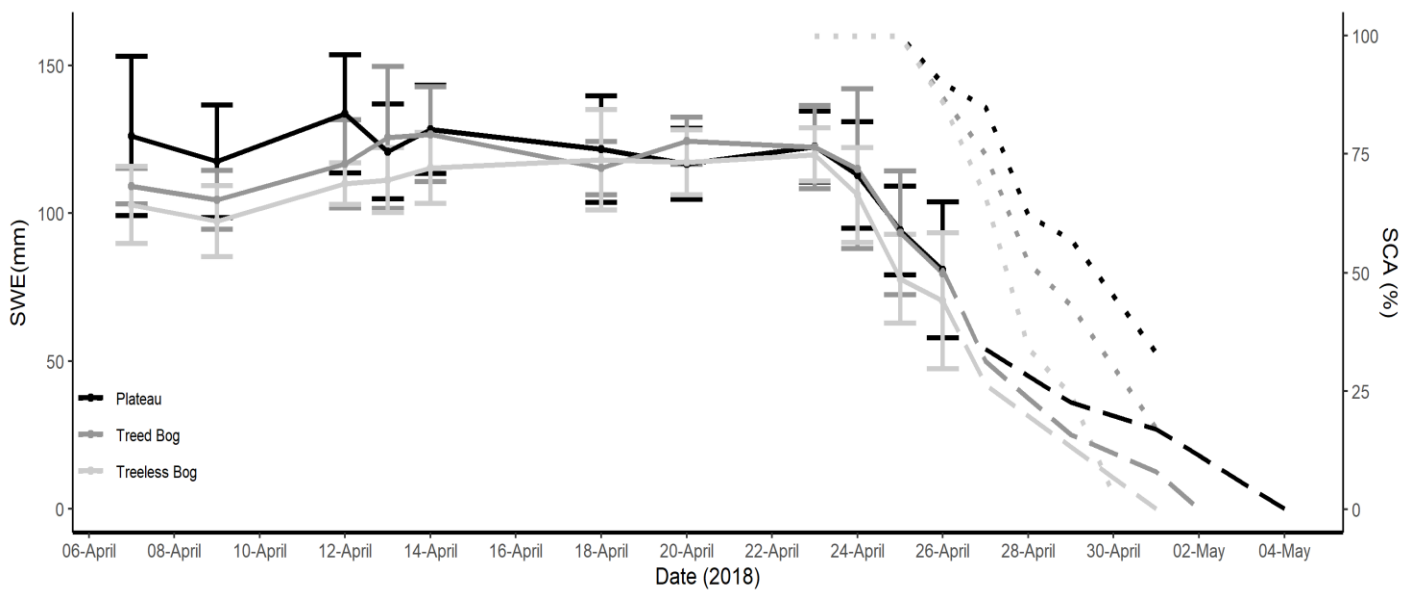


**Figure 3:** SWE and SCA measurements. SWE. Snowmelt commences on April 23<sup>rd</sup> and is denoted by the dotted line. Pre-melt measurements were taken for approximately 15 days, while melt measurements were taken for 5 days. The error bars represent the standard deviation of the average SWE measurement for each landcover type. After the final measurement (April 26<sup>th</sup>), linear interpolation was used to complete melt for each feature and is denoted with the dashed line. It should be noted that the snow-free day for each landcover type is approximated to  $\pm 1$  day using areal imagery and field notes, and. Snow covered area (SCA%) is plotted near the end of the period to depict the areal loss of the snowpack and is denoted by the dotted lines.

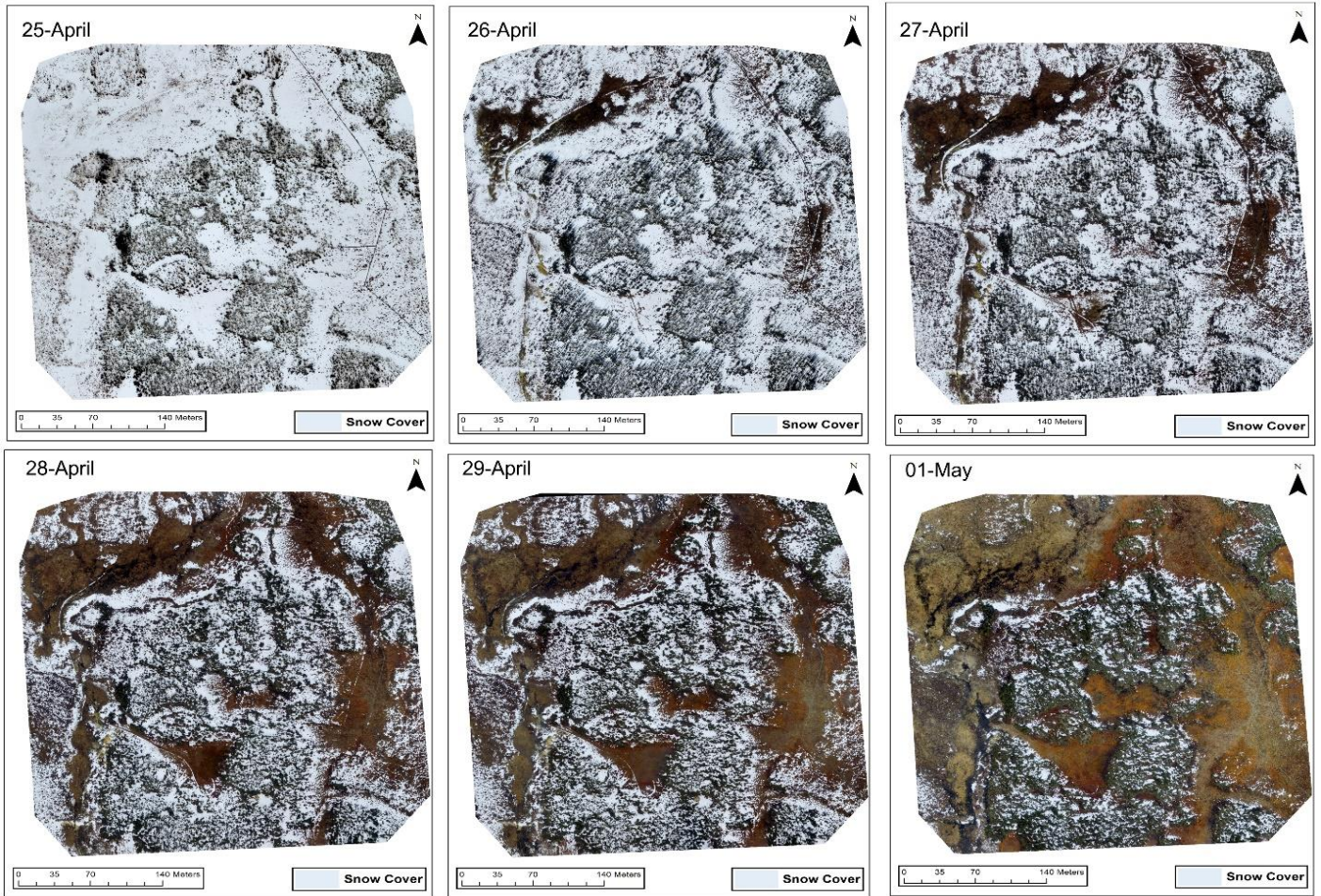


**Figure 4:** Mosaiced drone images of classified snow cover for three study sites throughout the snowmelt period. Images were captured daily and were classified using an iso cluster unsupervised image classification. Snow cover for each day is depicted in light blue. April 25<sup>th</sup> is the baseline for the analysis.

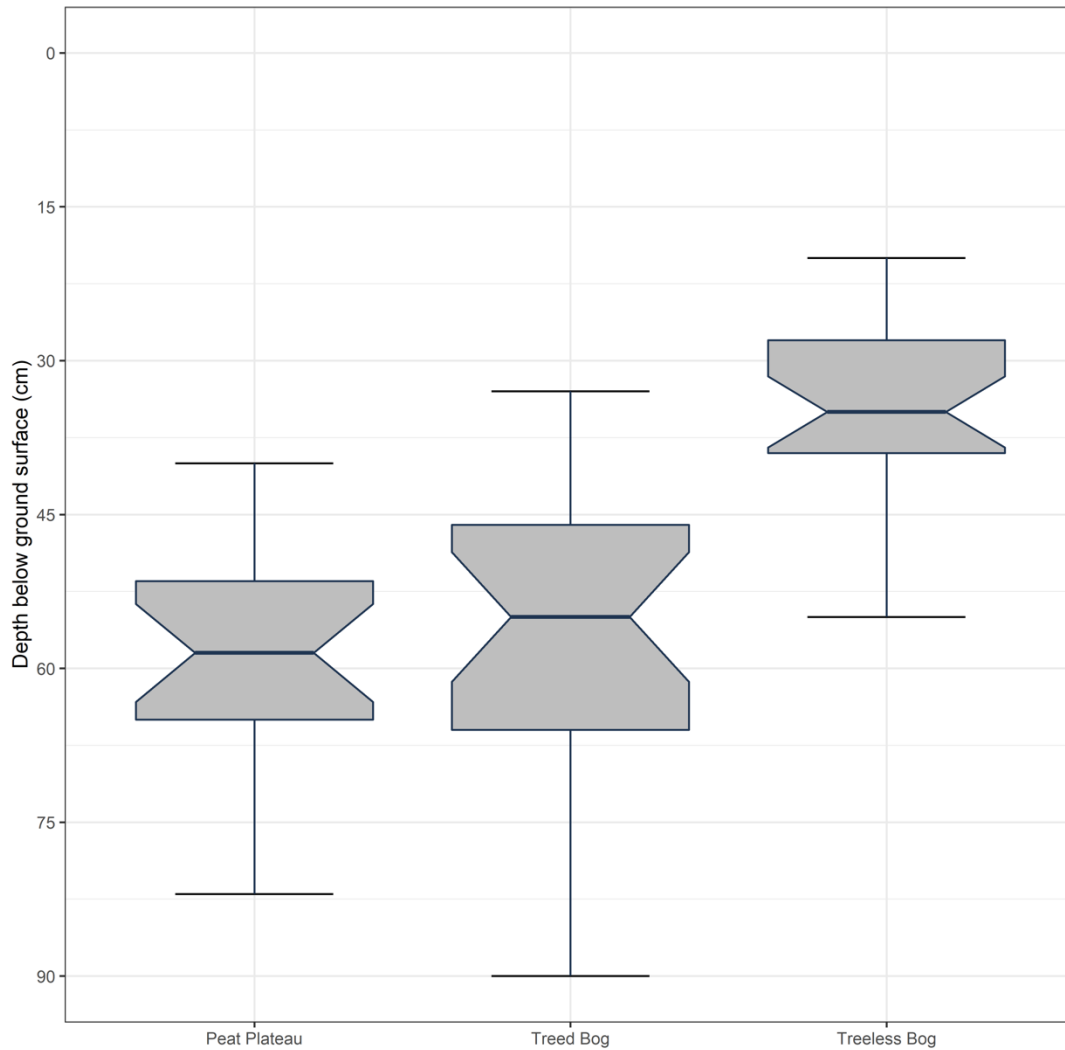


**Figure 5:** Thickness of seasonal frost for all three land cover types. Peat plateau and treed bog were not statistically different ( $p = 0.5$ ). The thickness of seasonal frost in the treeless bog had statistically significant ( $p < 0.05$ ) differences than the other two land cover types. The notches within each boxplot represents an approximate 95% confidence interval of the median. If the notches do not overlap, there is evidence of a statistically significant difference.

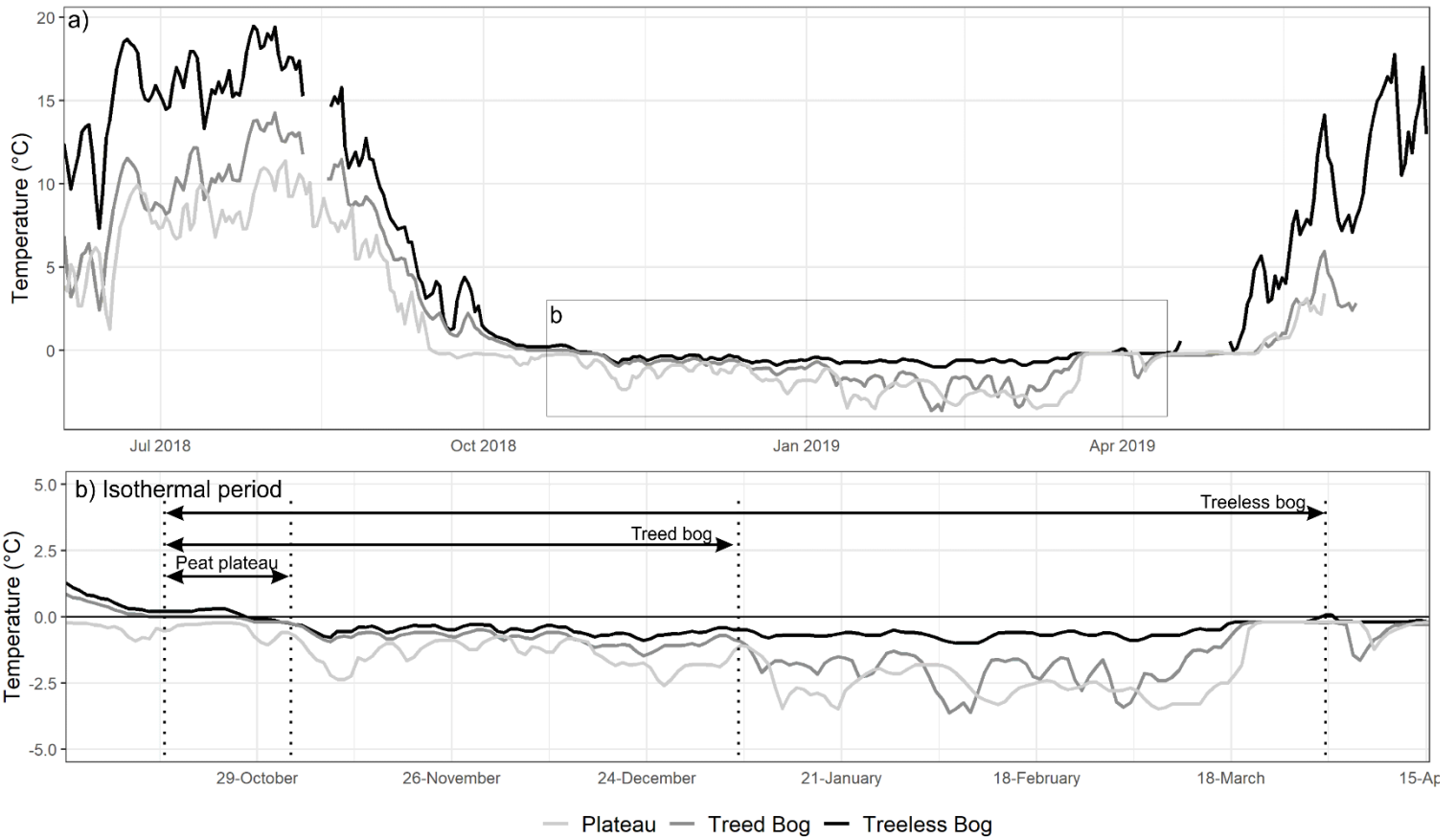


**Figure 6:** Daily ground temperature at 10cm depth at three locations within Site 1; b) Length of the isothermal period for each land cover type between October 2018 and April 2019. An offset was applied to each dataset to align the observed zero-curtain to the actual zero-curtain (-0.02°C).

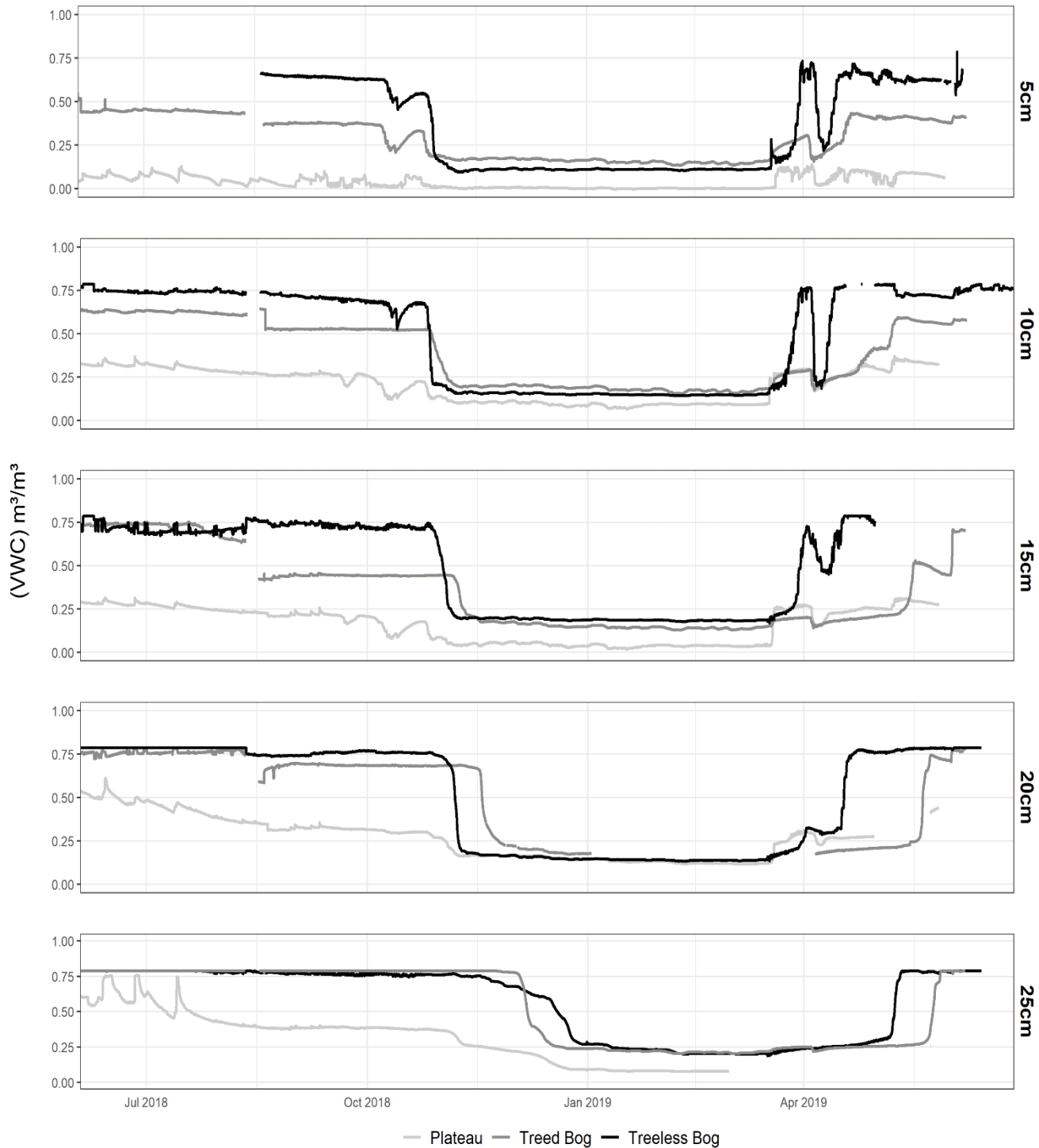


**Figure 7:** Continuous soil moisture VWC ( $\text{m}^3/\text{m}^3$ ) record at 5 discrete depth intervals (5cm, 10cm, 15cm, 20cm, 25cm, 30cm) for each landcover type. Data was collected for a year between June 2018 and June 2019. Data was removed at 5 cm from the treeless bog due to contact issues with the sensor, and the abrupt changes in VWC in mid-August occurred due to the sensors being disturbed and fixed less than a week later

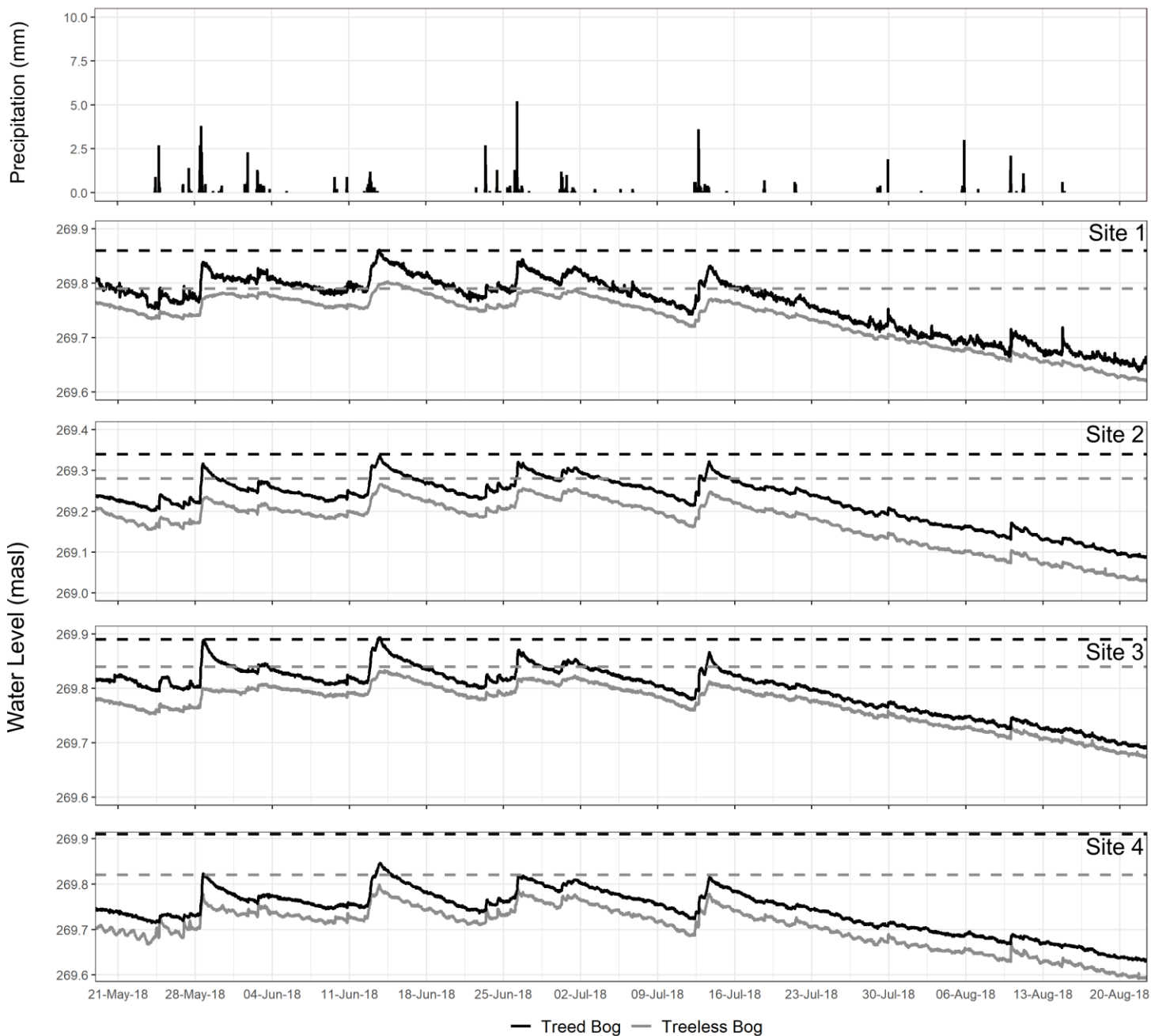
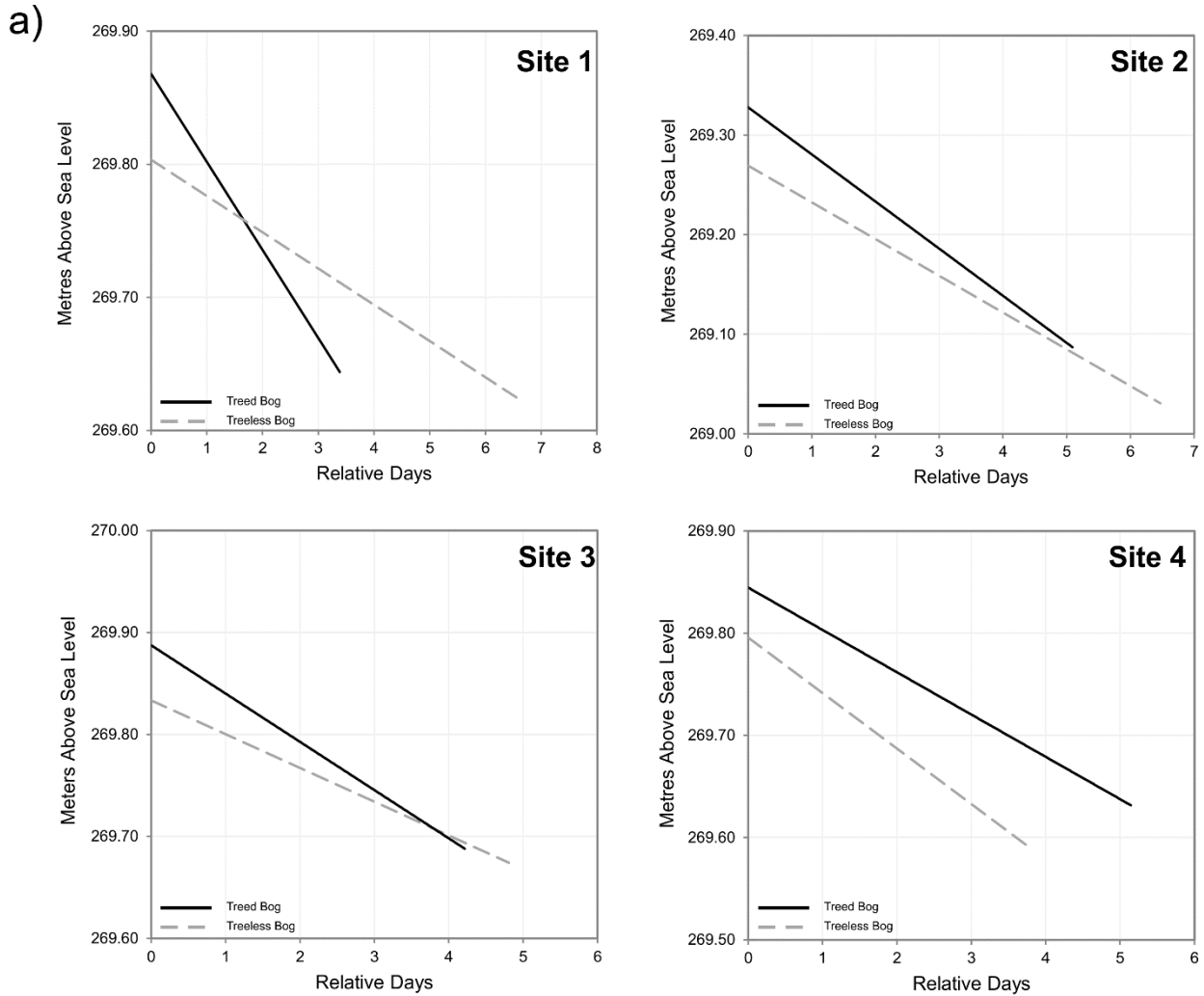


**Figure 8:** Mean water table measurements between May and June 2018 were recorded every 30-min at each well using a pressure transducer and are denoted as the solid line. The dotted line denotes the mean ground elevation ( $n = 4$ ) surrounding each corresponding well and was measured in the summer of 2018 using dGPS. Precipitation events (greater than 0.2mm) are depicted in the first plot. The average water table depth was 9 cm at the treeless bog wells and 12.5 cm at the treed bog wells



b)

Event	Precipitation (mm)	Treed Bog (day <sup>-1</sup> )	Treeless Bog (day <sup>-1</sup> )	Plateau (day <sup>-1</sup> )
1	22.5	0.00034	0.00019	0.000130
2	13.1	0.00033	0.00028	0.000155
3	15.0	0.00030	0.00025	0.000198
4	16.3	0.00033	0.00027	0.000207

**Figure 9:** a) Master recession curve trendlines for each treed and treeless bog well. The single peat plateau well was not plotted due differences in magnitude. b) A summary of each individual precipitation event and its corresponding mean recession coefficient for each landcover classification.

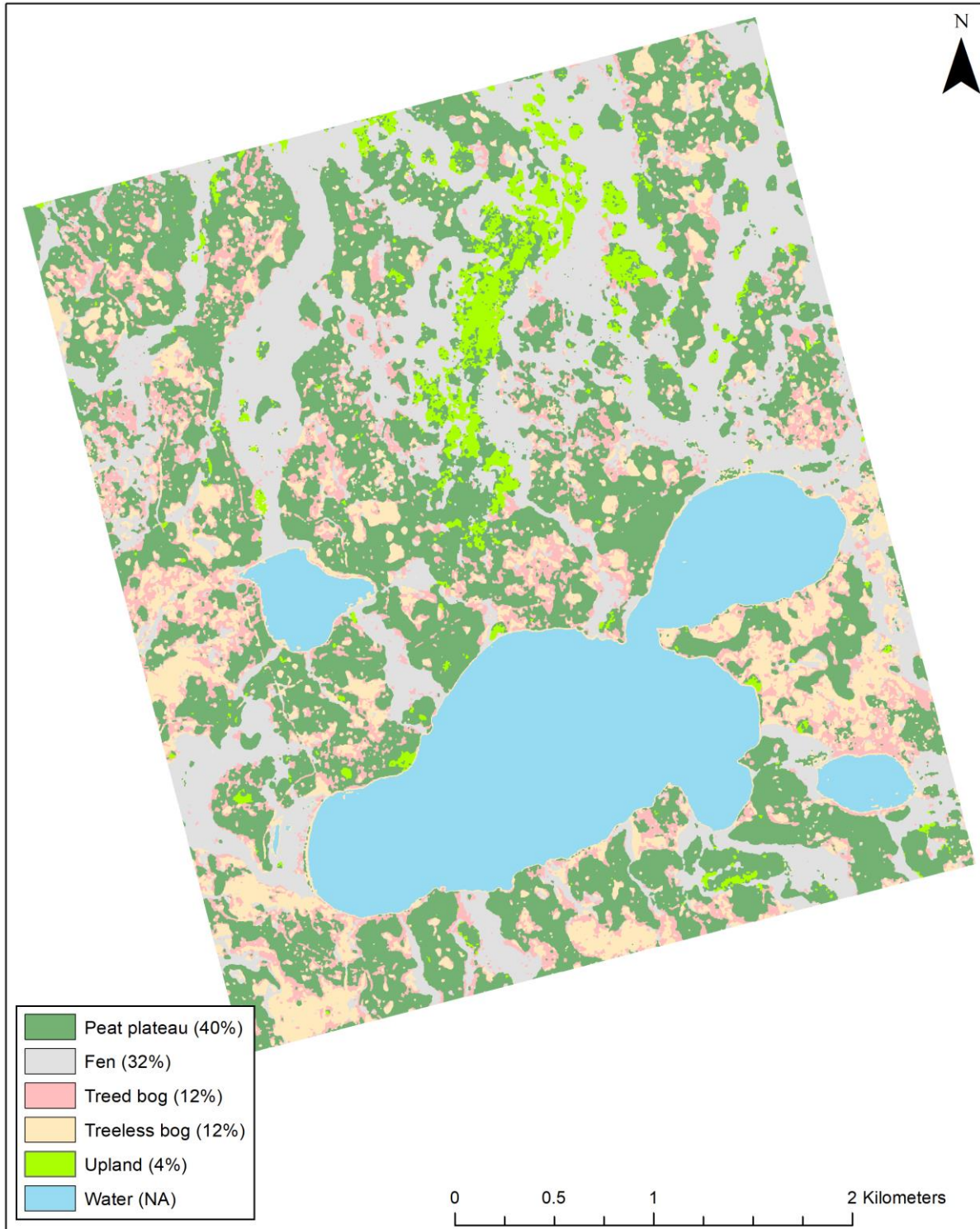


**Figure 10:** Supervised image classification of Scotty Creek within a small subset of the peatland portion of the basin. The classification was completed using Worldview-2 and LiDAR imagery.

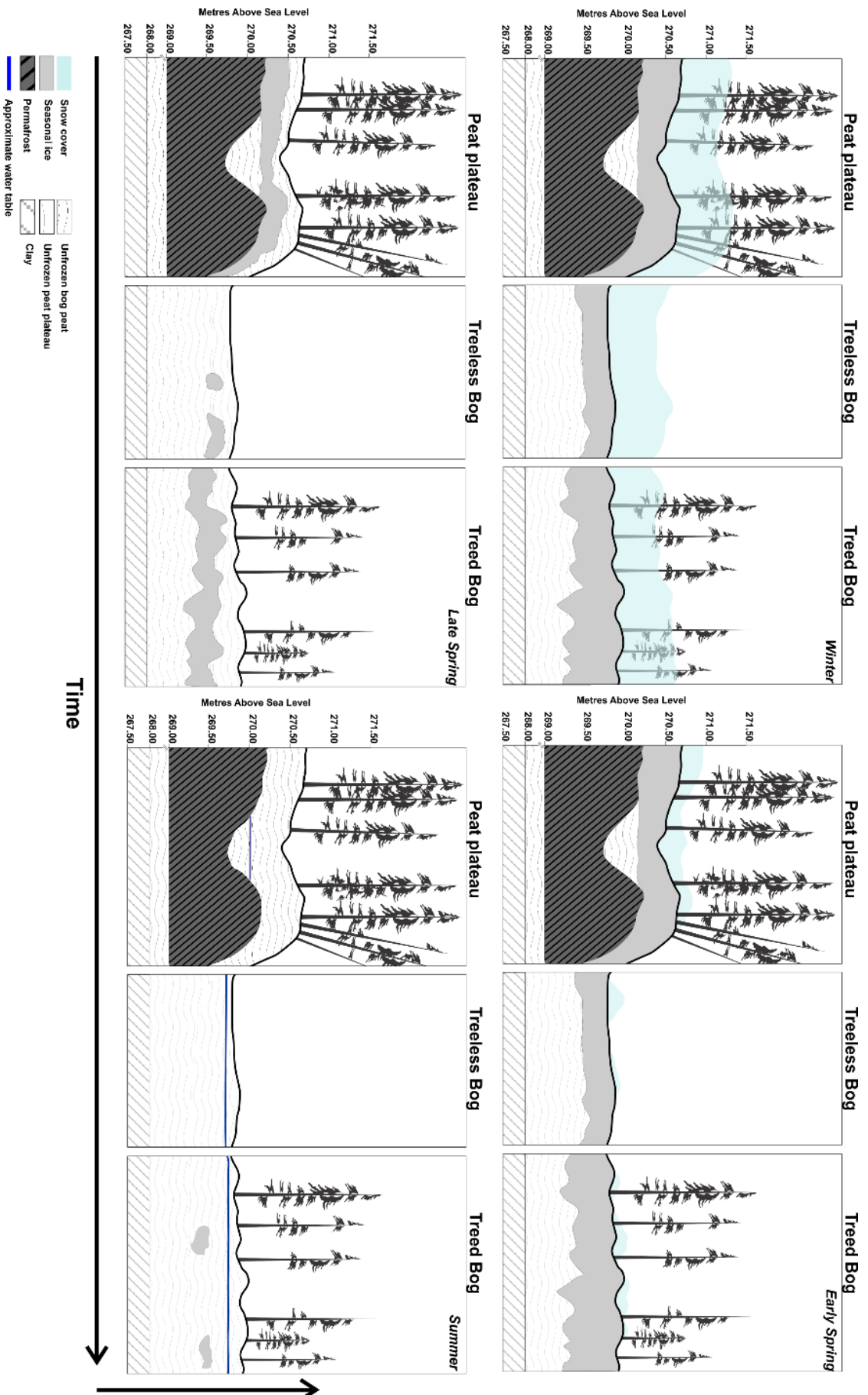


**Figure 11:** Conceptual diagram displaying differences in measured snow depth, depth of seasonal ice, and water table elevation between each landscape type, as well as the formation of treed bogs through both time and space. Currently, it is proposed that treed bogs form due to the upward growth of *Sphagnum* *sp.* and the gradual dewatering of landscapes. Each panel of the four panels represent the approximate season in which the data collection occurred. The arrow denoting time represents the temporal transition of landscapes, while the arrows depicting upward growth represents the spatial transition of treed bogs. All data was plotted relative to the ground elevation points.

## References

- Atchley, A.L., Coon, E.T., Painter, S.L., Harp, D.R. & Wilson, C.J. 2016. Influences and interactions of inundation, peat, and snow on active layer thickness. *Geophysical Research Letters* 43 : 5116–5123. DOI: 10.1002/2016GL068550
- Baltzer, J.L., Veness, T., Chasmer, L.E., Sniderhan, A.E. & Quinton, W.L. 2014. Forests on thawing permafrost: Fragmentation, edge effects, and net forest loss. *Global Change Biology* 20 : 824–834. DOI: 10.1111/gcb.12349
- Beilman, D.W. 2001. Plant community and diversity change due to localized permafrost dynamics in bogs of western Canada. *Canadian Journal of Botany* 79 : 983–993. DOI: 10.1139/cjb-79-8-983
- Beilman, D.W., Vitt, D.H. & Halsey, L.A. 2001. Localized Permafrost Peatlands in Western Canada: Definition, Distributions, and Degradation. *Arctic, Antarctic, and Alpine Research* 33 : 70. DOI: 10.2307/1552279
- Bourgault, M.A., Larocque, M. & Garneau, M. 2017. Quantification of peatland water storage capacity using the water table fluctuation method. *Hydrological Processes*. DOI: 10.1002/hyp.11116
- Brown, R.J.E. 1970. *Permafrost in Canada; its influence on Northern development*,
- Camill, P. 2000. How much do local factors matter for predicting transient ecosystem dynamics? Suggestions from permafrost formation in Boreal peatlands. *Global Change Biology*. DOI: 10.1046/j.1365-2486.2000.00293.x
- Camill, P. 1999. Peat accumulation and succession following permafrost thaw in the boreal peatlands of Manitoba, Canada. *Écoscience* 6 : 592–602. DOI: 10.1080/11956860.1999.11682561
- Camill, P. 2005. Permafrost thaw accelerates in boreal peatlands during late-20th century climate warming. *Climatic Change* 68 : 135–152. DOI: 10.1007/s10584-005-4785-y
- Camill, P., Lynch, J.A., Clark, J.S., Adams, J.B. & Jordan, B. 2001. Changes in biomass, aboveground net primary production, and peat accumulation following permafrost thaw in the boreal peatlands of Manitoba, Canada. *Ecosystems*. DOI: 10.1007/s10021-001-0022-3
- Carey, S.K. & Woo, M.K. 1999. Hydrology of two slopes in subarctic Yukon, Canada. *Hydrological Processes*. DOI: 10.1002/(SICI)1099-1085(199911)13:16<2549::AID-HYP938>3.0.CO;2-H
- Carey, S.K. & Woo, M.K. 2001. Slope runoff processes and flow generation in a subarctic, subalpine catchment. *Journal of Hydrology* 253 : 110–129. DOI: 10.1016/S0022-1694(01)00478-4
- Carpino, O.A., Berg, A.A., Quinton, W.L. & Adams, J.R. 2018. Climate change and permafrost thaw-induced boreal forest loss in northwestern Canada. *Environmental Research Letters* 13 : 084018. DOI: 10.1088/1748-9326/aad74e
- Carpino, O., Haynes, K., Connon, R., Craig, J., Devoie, É., Quinton, W. 2020. The trajectory of landcover change in the discontinuous permafrost zone, northwestern Canada. *In prep*

- Chasmer, L. & Hopkinson, C. 2016. Threshold loss of discontinuous permafrost and landscape evolution. *Global Change Biology* 23 : 2672–2686. DOI: 10.1111/gcb.13537
- Chasmer, L., Hopkinson, C. & Quinton, W. 2010. Quantifying errors in discontinuous permafrost plateau change from optical data, Northwest Territories, Canada: 1947-2008. *Canadian Journal of Remote Sensing*. DOI: 10.5589/m10-058
- Chasmer, L., Hopkinson, C., Veness, T., Quinton, W. & Baltzer, J. 2014. A decision-tree classification for low-lying complex land cover types within the zone of discontinuous permafrost. *Remote Sensing of Environment* 143 : 73–84. DOI: 10.1016/j.rse.2013.12.016
- Chasmer, L., Quinton, W., Hopkinson, C., Petrone, R. & Whittington, P. 2011. Vegetation Canopy and Radiation Controls on Permafrost Plateau Evolution within the Discontinuous Permafrost Zone, Northwest Territories, Canada. *Permafrost and Periglacial Processes* 22 : 199–213. DOI: 10.1002/ppp.724
- Connon, R., Devoie, É., Hayashi, M., Veness, T. & Quinton, W. 2018. The Influence of Shallow Taliks on Permafrost Thaw and Active Layer Dynamics in Subarctic Canada. *Journal of Geophysical Research: Earth Surface* 123 : 281–297. DOI: 10.1002/2017JF004469
- Connon, R.F., Quinton, W.L., Craig, J.R., Hanisch, J. & Sonnentag, O. 2015. The hydrology of interconnected bog complexes in discontinuous permafrost terrains. *Hydrological Processes* 29 : 3831–3847. DOI: 10.1002/hyp.10604
- Connon, R.F., Quinton, W.L., Craig, J.R. & Hayashi, M. 2014. Changing hydrologic connectivity due to permafrost thaw in the lower Liard River valley, NWT, Canada. *Hydrological Processes* 28 : 4163–4178. DOI: 10.1002/hyp.10206
- Devoie, É.G., Craig, J.R., Connon, R.F. & Quinton, W.L. 2019. Taliks: A Tipping Point in Discontinuous Permafrost Degradation in Peatlands. *Water Resources Research*. DOI: 10.1029/2018WR024488
- Davis, R.E., Hardy, J.P., Ni, W., Woodcock, C., McKenzie, J.C., Jordan, R. & Li, X. 1997. Variation of snow cover ablation in the boreal forest: A sensitivity study on the effects of conifer canopy. *Journal of Geophysical Research Atmospheres*. DOI: 10.1029/97jd01335
- Golding, D.L. & Swanson, R.H. 1986. Snow distribution patterns in clearings and adjacent forest. *Water Resources Research*. DOI: 10.1029/WR022i013p01931
- Gordon, J., Quinton, W., Branfireun, B.A. & Olefeldt, D. 2016. Mercury and methylmercury biogeochemistry in a thawing permafrost wetland complex, Northwest Territories, Canada. *Hydrological Processes*. DOI: 10.1002/hyp.10911
- Halsey, L.A., Vitt, D.H. & Zoltai, S.C. 1995. Disequilibrium response of permafrost in boreal continental western Canada to climate change. *Climatic Change* 30 : 57–73. DOI: 10.1007/BF01093225
- Harding, R.J. & Pomeroy, J.W. 1996. The energy balance of the winter boreal landscape. *Journal of Climate*. DOI: 10.1175/1520-0442(1996)009<2778:TEBOTW>2.0.CO;2
- Hardy, J.P., Melloh, R., Koenig, G., Marks, D., Winstal, A., Pomeroy, J.W. & Link, T. 2004. Solar radiation transmission through conifer canopies. *Agricultural and Forest Meteorology*. DOI: 10.1016/j.agrformet.2004.06.012
- Houghton, E. 2018. *Permafrost thaw-induced forest to wetland conversion : potential impacts on snowmelt and basin runoff in northwestern Canada* By.

- Hayashi, M., Quinton, W.L., Pietroniro, A. & Gibson, J.J. 2004. Hydrologic functions of wetlands in a discontinuous permafrost basin indicated by isotopic and chemical signatures. *Journal of Hydrology* 296 : 81–97. DOI: 10.1016/j.jhydrol.2004.03.020
- Haynes, K., Smart, J., Disher, B., Carpino, O., Quinton, W. 2020. The role of hummocks in re-establishing black spruce forest following permafrost thaw. *In prep.*
- Haynes, K.M., Connon, R.F. & Quinton, W.L. 2018. Permafrost thaw induced drying of wetlands at Scotty Creek, NWT, Canada. *Environmental Research Letters* 13 : 114001. DOI: 10.1088/1748-9326/aae46c
- Helbig, M., Pappas, C. & Sonnentag, O. 2016. Permafrost thaw and wildfire: Equally important drivers of boreal tree cover changes in the Taiga Plains, Canada. *Geophysical Research Letters*. DOI: 10.1002/2015GL067193
- Helbig, Manuel, Wischnewski, K., Kljun, N., Chasmer, L.E., Quinton, W.L., Detto, M. & Sonnentag, O. 2016. Regional atmospheric cooling and wetting effect of permafrost thaw-induced boreal forest loss. *Global Change Biology* 22 : 4048–4066. DOI: 10.1111/gcb.13348
- Ishikawa, M., Sharkhuu, N., Zhang, Y., Kadota, T. & Ohata, T. 2005. Ground thermal and moisture conditions at the southern boundary of discontinuous permafrost, Mongolia. *Permafrost and Periglacial Processes*. DOI: 10.1002/ppp.483
- Jeglum, J.K. & He Fangliang 1995. Pattern and vegetation-environment relationships in a boreal forested wetland in northeastern Ontario. *Canadian Journal of Botany*. DOI: 10.1139/b95-067
- Jorgenson, M.T. & Osterkamp, T.E. 2005. Response of boreal ecosystems to varying modes of permafrost degradation. *Canadian Journal of Forest Research* 35 : 2100–2111. DOI: 10.1139/x05-153
- Jorgenson, M.T., Romanovsky, V., Harden, J., Shur, Y., O'Donnell, J., Schuur, E.A.G., Kanevskiy, M. & Marchenko, S. 2010. Resilience and vulnerability of permafrost to climate change. *Canadian Journal of Forest Research* 40 : 1219–1236. DOI: 10.1139/X10-060
- Kettridge, N., Thompson, D.K., Bombonato, L., Turetsky, M.R., Benscoter, B.W. & Waddington, J.M. 2013. The ecohydrology of forested peatlands: Simulating the effects of tree shading on moss evaporation and species composition. *Journal of Geophysical Research: Biogeosciences* 118 : 422–435. DOI: 10.1002/jgrg.20043
- Kneisel, C. 2006. Assessment of subsurface lithology in mountain environments using 2D resistivity imaging. *Geomorphology* 80 : 32–44. DOI: 10.1016/j.geomorph.2005.09.012
- Kneisel, C., Hauck, C., Fortier, R. & Moorman, B. 2008. Advances in geophysical methods for permafrost investigations. *Permafrost and Periglacial Processes* 19 : 157–178. DOI: 10.1002/ppp.616
- Lafleur, P.M., Hember, R.A., Admiral, S.W. & Roulet, N.T. 2005. Annual and seasonal variability in evapotranspiration and water table at a shrub-covered bog in southern Ontario, Canada. *Hydrological Processes* 19 : 3533–3550. DOI: 10.1002/hyp.5842
- Lewkowicz, A.G., Etzelmüller, B. & Smith, S.L. 2011. Characteristics of discontinuous permafrost based on ground temperature measurements and electrical resistivity tomography, Southern Yukon, Canada. *Permafrost and Periglacial Processes* 22 : 320–342. DOI: 10.1002/ppp.703
- Lohila, A., Minkinen, K., Aurela, M., Tuovinen, J.P., Penttilä, T., Ojanen, P. & Laurila, T. 2011.

- Greenhouse gas flux measurements in a forestry-drained peatland indicate a large carbon sink. *Biogeosciences*. DOI: 10.5194/bg-8-3203-2011
- Mackay, J.R. 1972. The World Of Underground Ice. *Annals of the Association of American Geographers* 62 : 1–22. DOI: 10.1111/j.1467-8306.1972.tb00839.x
- Marks, D., Kimball, J., Tingey, D. & Link, T. 1998. The sensitivity of snowmelt processes to climate conditions and forest cover during rain-on-snow: a case study of the 1996 Pacific Northwest flood. *Hydrological Processes*. DOI: 10.1002/(SICI)1099-1085(199808/09)12:10/11<1569::AID-HYP682>3.0.CO;2-L
- McClymont, A.F., Hayashi, M., Bentley, L.R. & Christensen, B.S. 2013. Geophysical imaging and thermal modeling of subsurface morphology and thaw evolution of discontinuous permafrost. *Journal of Geophysical Research: Earth Surface* 118 : 1826–1837. DOI: 10.1002/jgrf.20114
- Menberu, M.W., Tahvanainen, T., Marttila, H., Irannezhad, M., Ronkanen, A.K., Penttinen, J. & Kløve, B. 2016. Water-table-dependent hydrological changes following peatland forestry drainage and restoration: Analysis of restoration success. *Water Resources Research*. DOI: 10.1002/2015WR018578
- Murphy, M., Laiho, R. & Moore, T.R. 2009. Effects of Water Table Drawdown on Root Production and Aboveground Biomass in a Boreal Bog. *Ecosystems* 12 : 1268–1282. DOI: 10.1007/s10021-009-9283-z
- Nathan, R.J. & McMahon, T.A. 1990. Evaluation of automated techniques for base flow and recession analyses. *Water Resources Research*. DOI: 10.1029/WR026i007p01465
- Nguyen, T.N., Burn, C.R., King, D.J. & Smith, S.L. 2009. Estimating the extent of near-surface permafrost using remote sensing, Mackenzie Delta, Northwest Territories. *Permafrost and Periglacial Processes*. DOI: 10.1002/ppp.637
- Osterkamp, T.E. & Romanovsky, V.E. 1999. Evidence for warming and thawing of discontinuous permafrost in Alaska. *Permafrost and Periglacial Processes* 10 : 17–37. DOI: 10.1002/(SICI)1099-1530(199901/03)10:1<17::AID-PPP303>3.0.CO;2-4
- Pastick, N.J., Jorgenson, M.T., Wylie, B.K., Nield, S.J., Johnson, K.D. & Finley, A.O. 2015. Distribution of near-surface permafrost in Alaska: Estimates of present and future conditions. *Remote Sensing of Environment*. DOI: 10.1016/j.rse.2015.07.019
- Payette, S., Delwaide, A., Caccianiga, M. & Beauchemin, M. 2004. Accelerated thawing of subarctic peatland permafrost over the last 50 years. *Geophysical Research Letters* 31 : 1–4. DOI: 10.1029/2004GL020358
- Pellerin, S. & Lavoie, C. 2000. Peatland fragments of southern Quebec: Recent evolution of their vegetation structure. *Canadian Journal of Botany*. DOI: 10.1139/b99-186
- Pelletier, N., Talbot, J., Olefeldt, D., Turetsky, M., Blodau, C., Sonnentag, O. & Quinton, W.L. 2017. Influence of Holocene permafrost aggradation and thaw on the paleoecology and carbon storage of a peatland complex in northwestern Canada. *The Holocene* 095968361769389. DOI: 10.1177/0959683617693899
- Pomeroy, J.W., Gray, D.M., Hedstrom, N.R. & Janowicz, J.R. 2002. Prediction of seasonal snow accumulation in cold climate forests. *Hydrological Processes* 16 : 3543–3558. DOI: 10.1002/hyp.1228

- Posavec, K., Bačani, A. & Nakić, Z. 2006. A visual basic spreadsheet macro for recession curve analysis. *Ground Water*. DOI: 10.1111/j.1745-6584.2006.00226.x
- Price, J.S., Heathwaite, A.L. & Baird, A.J. 2003. Hydrological processes in abandoned and restored peatlands: An overview of management approaches. In *Wetlands Ecology and Management*. DOI: 10.1023/A:1022046409485
- Quinton, W., Berg, A., Braverman, M., Carpino, O., Chasmer, L., Connon, R., Craig, J., Devoie, É., Hayashi, M., Haynes, K., Olefeldt, D., Pietroniro, A., Rezanezhad, F., Schincariol, R. & Sonnentag, O. 2019. A synthesis of three decades of hydrological research at Scotty Creek, NWT, Canada. *Hydrology and Earth System Sciences* 23 : 2015–2039. DOI: 10.5194/hess-23-2015-2019
- Quinton, W.L. & Connon, R.F. 2017. Toward Understanding the Trajectory of Hydrological Change in the Southern Taiga Plains , NWT , Canada. 1–10.
- Quinton, W.L. & Gray, D.M. 2003. Subsurface drainage from organic soils in permafrost terrain : the major factors to be represented in a runoff model. *Proceedings of the Eighth International Conference on Permafrost*.
- Quinton, W.L., Hayashi, M. & Chasmer, L.E. 2009. Peatland Hydrology of Discontinuous Permafrost in the Northwest Territories : Overview and Synthesis. *Canadian Water Resources Journal* 34 : 311–328.
- Quinton, W.L., Hayashi, M. & Chasmer, L.E. 2011. Permafrost-thaw-induced land-cover change in the Canadian subarctic: Implications for water resources. *Hydrological Processes* 25 : 152–158. DOI: 10.1002/hyp.7894
- Quinton, W.L., Hayashi, M. & Pietroniro, A. 2003. Connectivity and storage functions of channel fens and flat bogs in northern basins. *Hydrological Processes* 17 : 3665–3684. DOI: 10.1002/hyp.1369
- Robinson, S.D. & Moore, T.R. 2000. The influence of permafrost and fire upon carbon accumulation in high boreal peatlands, Northwest Territories, Canada. *Arctic, Antarctic and Alpine Research* 32 : 155–166. DOI: 10.2307/1552447
- Shur, Y.L. & Jorgenson, M.T. 2007. Patterns of permafrost formation and degradation in relation to climate and ecosystems. *Permafrost and Periglacial Processes* 18 : 7–19. DOI: 10.1002/ppp.582
- Sicart, J.E., Essery, R.L.H., Pomeroy, J.W., Hardy, J., Link, T. & Marks, D. 2004. A Sensitivity Study of Daytime Net Radiation during Snowmelt to Forest Canopy and Atmospheric Conditions. *Journal of Hydrometeorology*. DOI: 10.1175/1525-7541(2004)005<0774:ASSODN>2.0.CO;2
- Tallaksen, L.M. 1995. A review of baseflow recession analysis. *Journal of Hydrology*. DOI: 10.1016/0022-1694(94)02540-R
- Tarnocai, C. 2009. The Impact of Climate Change on Canadian Peatlands. *Canadian Water Resources Journal* 34 : 453–466. DOI: 10.4296/cwrj3404453
- Thie, J. 1974. Distribution and Thawing of Permafrost in the Southern Part of the Discontinuous Permafrost Zone in Manitoba. 27 : 189–200.
- Turetsky, M.R., Wieder, R.K., Vitt, D.H., Evans, R.J. & Scott, K.D. 2007. The disappearance of relict permafrost in boreal north America: Effects on peatland carbon storage and fluxes. *Global*

*Change Biology*. DOI: 10.1111/j.1365-2486.2007.01381.x

Turetsky, M.R., Wieder, R.K., Williams, C.J. & Vitt, D.H. 2000. Organic matter accumulation, peat chemistry, and permafrost melting in peatlands of boreal Alberta. *Écoscience*. DOI: 10.1080/11956860.2000.11682608

Tutubalina, O. V. & Rees, W.G. 2001. Vegetation degradation in a permafrost region as seen from space: Noril'sk (1961-1999). *Cold Regions Science and Technology*. DOI: 10.1016/S0165-232X(01)00049-0

Vitt, D.H., Halsey, L.A. & Zoltai, S.C. 1994. The Bog Landforms of Continental Western Canada in Relation to Climate and Permafrost Patterns. *Arctic and Alpine Research* 26 : 1. DOI: 10.2307/1551870

Waddington, J.M., Morris, P.J., Kettridge, N., Granath, G., Thompson, D.K. & Moore, P.A. 2015. Hydrological feedbacks in northern peatlands. *Ecohydrology* 8 : 113–127. DOI: 10.1002/eco.1493

Walvoord, M.A. & Kurylyk, B.L. 2016. Hydrologic Impacts of Thawing Permafrost—A Review. *Vadose Zone Journal* 15 : 0. DOI: 10.2136/vzj2016.01.0010

Warren, R.K., Pappas, C., Helbig, M., Chasmer, L.E., Berg, A.A., Baltzer, J.L., Quinton, W.L. & Sonnentag, O. 2018. Minor contribution of overstorey transpiration to landscape evapotranspiration in boreal permafrost peatlands. *Ecohydrology* 11 : e1975. DOI: 10.1002/eco.1975

Woo, M.-K., Kane, D.L., Carey, S.K. & Yang, D. 2008. Progress in permafrost hydrology in the new millennium. *Permafrost and Periglacial Processes* 19 : 237–254. DOI: 10.1002/ppp.613

Wright, N., Hayashi, M. & Quinton, W.L. 2009. Spatial and temporal variations in active layer thawing and their implication on runoff generation in peat-covered permafrost terrain. *Water Resources Research* 45 : 1–13. DOI: 10.1029/2008WR006880

Wright, N., Quinton, W.L. & Hayashi, M. 2008. Hillslope runoff from an ice-cored peat plateau in a discontinuous permafrost basin, Northwest Territories, Canada. *Hydrological Processes* 22 : 2816–2828. DOI: 10.1002/hyp.7005

Wu, J., Kutzbach, L., Jager, D., Wille, C. & Wilmking, M. 2010. Evapotranspiration dynamics in a boreal peatland and its impact on the water and energy balance. *Journal of Geophysical Research: Biogeosciences* 115 : 1–18. DOI: 10.1029/2009JG001075

Zhang, T. 2005. Influence of the seasonal snow cover on the ground thermal regime: An overview. *Reviews of Geophysics* 43 : RG4002. DOI: 10.1029/2004RG000157

Zoltai, S.C. 1993. Cyclic Development of Permafrost in the Peatlands of Northwestern Canada. *Arctic and Alpine Research* 25 : 240–246. DOI: 10.2307/1551820

Zoltai, S.C. 1972. Palsas and Peat Plateaus in Central Manitoba and Saskatchewan. *Canadian Journal of Forest Research* 2 : 291–302. DOI: 10.1139/x72-046

Zoltai, S.C. 1995. Permafrost Distribution in Peatlands of West-Central Canada during the Holocene Warm Period 6000 Years BP. *Geographie physique Et Quaternaire* 49 : 45–54. DOI: 10.7202/033029ar

Zoltai, S.C. & Tarnocai, C. 1975. Perennially Frozen Peatlands in the Western Arctic and Subarctic of Canada. *Canadian Journal of Earth Sciences*. DOI: 10.1139/e75-004

## **Appendix A:** Additional information on methods

### **Site selection and methodology**

To determine additional study sites within Scotty Creek (Sites 2 – 4), a supervised image classification was created using multi-spectral Worldview-2 imagery. A maximum-likelihood algorithm classification was created using ArcGIS, and a small number of training sites were used for each landcover type ( $n = 5$ ). This initial classification served as a tool to determine other sites within the study area that may be considered treed bog based on their spectral properties, as these sites could not be assessed in person due to logistical constraints, and as such, no accuracy assessment was completed on this classification. LiDAR products such as digital elevation models (DEM) and canopy height models (CHM) were also used to determine areas that were both low elevation and treed. Sites were not selected to achieve wide-spread spatial representation throughout the small AOI (area of interest), but instead were selected based on a combination of the classification and closeness to other sites within Scotty Creek. A geophysical investigation was conducted at all four study sites to gain a more thorough understanding of subsurface properties. Only the ERT (electrical resistivity tomography) measurements will be presented here.

### **Snowpack Characteristics**

Due to drone flights occurring at different times throughout the day, shadows are present during some of the images. To deal with this discrepancy, three classes were used to classify the shadows as snow cover for the first three days of analysis. After this point, two classes were selected to represent 'snow-cover' and 'snow-free' area. In total, 50 random points were distributed based on stratified random sampling, where the points were randomly distributed

within each class with an equal number of points (n=25) in each class. Points were then verified as either 'snow-covered' or 'snow-free' based on visual observation of each SCA drone image.

### **Seasonal ground freeze and thaw**

End of summer thaw depth measurements were conducted on the portion of transects that crossed peat plateaux and was used to determine the extent of the active layer when it reaches its maximum thaw depth. These measurements are completed similarly to depth of refreeze, but the frost probe is inserted into the ground until it reaches the frost table and cannot penetrate any further. Ground temperature and soil moisture were measured using five temperature-moisture (TM) probes connected to data loggers (EM50, METER Environment, USA), but because the primary purpose of these probes is to measure soil moisture, the accuracy of the temperature measurements is  $\pm 1^{\circ}\text{C}$ . An offset was applied to each dataset to align the observed zero-curtain to the actual zero-curtain ( $-0.02^{\circ}\text{C}$ ) commonly observed by other cold regions studies (Woo 2012; Quinton & Baltzer 2013).

### **Water level fluctuations and hydrograph recession**

For the well installations, a black iron pipe was installed adjacent to each PVC pipe into the underlying mineral soil (~2 – 3 m below the surface) and was used as an anchor point for the pressure transducer. These anchor points were installed to prevent the vertical movement of the transducer due to heaving of the peat surface throughout the summer months. A measurement of the well casing, top of Anchor point, and water table was taken, as well as five measurements of the ground surface surrounding the well. To determine water level, Barometric pressure was collected within 1 km of the study site and was subtracted from the total pressure to provide a depth of water above the pressure transducer in the well.

Typically, Recession analyses will evaluate the recession of the hydrography until baseflow conditions are met on the hydrograph. Because this analysis was conducted in

peatlands, a baseflow condition could not be adequately established and as such, the recession limb for each land cover feature was evaluated for 5 days or up to the following precipitation event. In total, four precipitation events (>10 mm) were examined for the analysis and are summarized in Figure 9. To create MRC curves, an adapted match stripping method was used, such that recession segments are superimposed into overlapping segments, resulting in a general characterization of water table recession for each landcover type at all four sites (Posavec et al. 2006).

### **Image classification and analysis**

To distinguish topographically elevated landscapes, the mean of the TPI product (0.100076) was used to determine the cut-off between high and low elevation features. A TPI value greater than the mean was classified as 'high elevation' and everything below this threshold was classified as 'low elevation'. Thresholds for both canopy gap fraction and canopy height were both determined iteratively using manual interpretation of the imagery. For example, the upland regions had both taller and more dense canopies characteristics and were therefore assigned higher canopy and gap fraction thresholds. Treeless bogs have very little canopy cover, and the CHM and gap fraction characteristics determined to reflect these characteristics. A similar process was used for both peat plateaux and treed bogs. The classification for fens and treed bogs relied on spectral properties, as the canopy and topographic characteristics were difficult to discern from other landcover types. The classification of a small portion of upland was weighted towards canopy characteristics as it was difficult to characterize topographically. To complete the accuracy assessment, a set of random points were generated for each landcover class and were verified using a combination of ground truth data and visual observations of high-quality areal imagery. The results of the matrix were then evaluated for overall accuracy and misclassification rates. Additionally, Cohen's Kappa was used to determine how the classification performed in comparison to chance.

## **Appendix B:** Additional discussion

### **Snowpack Characteristics**

In a dense stand of boreal black spruce (*Picea mariana*) trees, snow accumulation is typically lower beneath the canopy (Pomeroy et al. 2002), but this effect is dependent on the effective Leaf Area Index (LAI) of the cover. For example, Baltzer et al. (2014) measured the effective LAI of peat plateaux to investigate thermal implications of radiation on ground thaw, and measured an effective LAI ranging between 0.8 and 2.0 depending on the distance from the plateau-wetland interface, while a black spruce canopy studied by Pomeroy et al. (2002) in Prince Albert Model Forest (Saskatchewan, Canada) had an effective LAI of 4.1. Because of the lower effective LAI of the black spruce forest studied here, accumulation of SWE is higher than forests in other regions with a denser forest canopy. The presence of canopy strongly influences the melt of a snowpack, as it reduces both turbulent fluxes as well as radiative fluxes. For example, Harding & Pomeroy (1996) found reported far lower incoming shortwave radiation below a dense pine canopy, as well as reductions in turbulent fluxes that would typically result in sublimation and redistribution of the snowpack. As the LAI of a forest increases, there is a steady decline in the amount of snowmelt energy reaching the snowpack and a resultant decrease in the snowmelt rate (Sicart et al. 2004). Although reductions in shortwave radiation and subsequent reductions in melt rate are the dominant trend, longwave radiation increases may offset reductions in shortwave irradiance, this effect is known as the 'radiative paradox' (Ambach 1974; Giesbrecht & Woo 2000; Pomeroy et al. 2009). Despite this, studies have noted the contribution of longwave radiation, but shortwave reductions and reduced melt remain the dominant trend for snowmelt below canopies (Haughton 2018; Link & Marks 1999).

Overall, the unsupervised classification accurately classified 'snow-free' and 'snow-covered' areas (Figure 4). The overall accuracy on 25-Apr was 88% (Kappa = 0.76) and

increased to 98% for the remaining classified images (Appendix E). For example, the overall accuracy on 25-Apr was 88% (Kappa = 0.76), and then increased to 98% on 26-Apr (Kappa = 0.96) and remained that accurate for the 27-Apr, 28-Apr, and 01-May classified images (Appendix E). The lower accuracies on 25-Apr favored type I error, where darker snow cover surrounding the base of some trees were classified as 'snow-free' when they were instead 'snow-cover'. This error only persisted for the first classified image. It should be noted that additional error rates may also be introduced due to the presence of snow cover beneath the black spruce crowns as this snow cover would not be visible in the images. Although this error may be negligible, it may result in under-represented SCA estimates within treed areas of the classification. Before snowmelt intensified, SCA was similar at all site types. Due to windy weather conditions, UAV flights could only be completed between 23-Apr and 01-May, and snowmelt had completed by 04-May.

### **Water level fluctuations and hydrograph recession**

Although ET was not directly measured in this study, the difference in ET between open bogs and a treed landscape can be significant (Warren et al. 2018), and may be influenced by factors such as canopy cover and the depth of the water table below the moss surface (Lafleur 2008; Hayward & Clymo 1982; Lafleur et al. 2005; Kellner 2001). For example, ET flux from a black spruce canopy can be significantly lower than surrounding wetland environments due to the considerably lower photosynthetic and transpiration rates of black spruce (Warren et al. 2018; Strilesky & Humphreys 2012; Murphy et al. 2009). Although ET was not measured for this study, ET contributions from black spruce within Scotty Creek are generally poor due to moisture availability and nutrient poor conditions on peat plateaux resulting in low productivity. For example, Warren et al. (2018) found lower ET rates within peat plateaux compared to Sphagnum dominated open bogs. This effect is compounded as plateaux degrade and the rooting zone floods, causing further reductions to productivity (Baltzer et al., 2014; Patankar et

al., 2015). Studies in temperate peatlands have noted similar findings. For example, Strilesky and Humphreys (2012) assessed ET between a temperate treed and open bog near Ottawa, Ontario for an entire hydrological year and demonstrated lower ET rates in the treed bog compared to the treeless portion of the same bog. This effect was most pronounced in the summer months when the water table (and moisture availability) was the lowest.

### **Image classification and analysis**

The classification performed most well when classifying fens and peat plateaux, with accuracies ranging between 97% and 93%. The classification for fens favored type I errors, where at times treeless bogs were classified as fens. Similarly, peat plateau's also favored type I errors.

Treeless bogs had higher accuracies that ranged between 94% to 67%. The classification of treeless bogs was most susceptible to type II errors, where other landcover types were misclassified as treeless bog. The classification performed well when classifying treed bogs as the accuracies were between 81% and 68%, which favored Type II errors, as other landscapes such as treeless bogs and fens would sometimes be misclassified as treed bogs. Although the classification performed well, the accuracy assessment utilized points rather than defined areas, which would introduce further bias into the accuracy assessment of the classification, as any misclassifications surrounding the boundaries of features or any misclassifications that didn't overlap with that specific point would not have been captured. For example, despite the uplands appearing to have high accuracies (between 100% to 71%), the placement of random accuracy assessment points may have not captured the true error in the classification of this landcover. This bias would have been compounded by the small area of upland relative to other landcover types within the AOI. Therefore, these accuracy assessments should be regarded with caution. Unfortunately, due to logistical constraints, the uplands within the northern part of the AOI could not be ground verified.

**Appendix C:** Statistical analysis of SWE, depth of refreeze and slope recession analysis. All tests were run at a 95% confidence interval.

Variable	Landcover	Residual df	F-value	P-value
<b>SWE – April 7<sup>th</sup></b>				
	<b>ANOVA</b>	15	3.081	0.0757
	treed bog – plateau			0.3201
	treeless bog – plateau			<b>0.0643</b>
	treeless bog – treed bog			0.6085
<b>SWE – April 26<sup>th</sup></b>				
	<b>ANOVA</b>	15	0.554	0.5860
	treed bog – plateau			0.5682
	treeless bog – plateau			0.7714
	treeless bog – treed bog			0.9382
<b>Depth of Refreeze</b>				
	<b>ANOVA</b>	67	37.34	< <b>0.001</b>
	treed bog – plateau			0.5680
	treeless bog – plateau			< <b>0.001</b>
	treeless bog – treed bog			< <b>0.001</b>
<b>Slope Recession</b>				
	<b>ANOVA</b>	30	18.4	< <b>0.001</b>
	treed bog – treeless bog			< <b>0.001</b>

**Appendix D:** Topographic, canopy, and spectral thresholds used for each landcover type within the image classification. Variables with dashes were not used to classify that landcover.

	<b>Peat plateau</b>	<b>Fen</b>	<b>Treed Bog</b>	<b>Treeless Bog</b>	<b>Upland</b>
<b>Topographic position index</b>	> 0.100076	≤ 0.100076	≤ 0.100076	≤ 0.100076	
<b>Canopy height</b>	> 1.2 m and ≤ 7 m	≤ 3.6 m	> 1.2 m and ≤ 7 m	≤ 1.2 m	≥ 7 m
<b>Canopy gap fraction</b>	0.61 – 0.96	0.96 – 1	0.61 – 0.96	0.96 – 1	< 0.61
<b>Spectral classes</b>	25	25	10	25	

**Appendix E:** Confusion matrices of predicted 'snow-free' and 'snow-covered' area compared to actual 'snow-free' and 'snow-covered' area of all drone images used for the SCA analysis. Classification accuracies are presented with overall accuracy, misclassification rate, and Kohen's Kappa.

**25-Apr**

		Predicted			
		Snow-free	Snow-cover	Total	
Actual	n=50				
	Snow-free	19	6	25	76
	Snow-cover	0	25	25	1
		100	81		

Overall Accuracy: 88%

Misclassification: 12%

Kohen's Kappa: 0.76

**28-Apr**

		Predicted			
		Snow-free	Snow-cover	Total	
Actual	n=50				
	Snow-free	24	1	25	96
	Snow-cover	0	25	25	1
		100	96		

Overall Accuracy: 98%

Misclassification: 2%

Kohen's Kappa: 0.98

**26-Apr**

		Predicted			
		Snow-free	Snow-cover	Total	
Actual	n=50				
	Snow-free	24	1	25	96
	Snow-cover	0	25	25	1
		100	96		

Overall Accuracy: 98%

Misclassification: 2%

Kohen's Kappa: 0.98

**29-Apr**

		Predicted			
		Snow-free	Snow-cover	Total	
Actual	n=50				
	Snow-free	22	3	25	88
	Snow-cover	0	25	25	1
		100	89		

Overall Accuracy: 94%

Misclassification: 6%

Kohen's Kappa: 0.88

**27-Apr**

		Predicted			
		Snow-free	Snow-cover	Total	
Actual	n=50				
	Snow-free	24	1	25	96
	Snow-cover	0	25	25	1
		100	96		

Overall Accuracy: 98%

Misclassification: 2%

Kohen's Kappa: 0.98

**01-May**

		Predicted			
		Snow-free	Snow-cover	Total	
Actual	n=50				
	Snow-free	24	1	25	96
	Snow-cover	0	25	25	1
		100	96		

Overall Accuracy: 98%

Misclassification: 2%

Kohen's Kappa: 0.98

**Appendix F:** Confusion matrix of predicted landcover type compared to actual landcover type within the classification AOI. Classification accuracies are presented with overall accuracy, misclassification rate, and Kohen's Kappa.

**Actual**

n = 251		Peat plateau	Fen	Treed bog	Treeless bog	Upland	Total	<b>Accuracy</b>
<b>Predicted</b>	Peat Plateau	85	2	7	2	4	100	85
	Fen	0	65	4	10	0	69	83
	Treed bog	3	1	25	2	0	31	81
	Treeless bog	0	1	1	29	0	31	94
	Upland	0	0	0	0	10	10	1
	Total	88	37	69	43	14		
<b>Accuracy</b>	97	94	68	67	71			

<b>Overall Accuracy: 85.3 %</b>
<b>Misclassification: 14.7 %</b>
<b>Kohen's Kappa: 0.79</b>

**Appendix G:** Discrete soil moisture points collected between 14-May and 01-June for each landcover type (n=20). Data was collected with a hydrosense-2 handheld soil moisture probe.

